January 31, 1965

Final Report

ELECTRICAL EFFECTS OF SHOCK WAVES: CONDUCTIVITY IN CsI, KI, AND NaCL.

Prepared for:

BALLISTIC RESEARCH LABORATORIES
ABERDEEN PROVING GROUND
MARYLAND

CONTRACT DA-04-200-ORD-1279

STANFORD RESEARCH INSTITUTE

MENLO PARK, CALIFORNIA

*SRI

STANFORD RESEARCH INSTITUTE
MENLO PARK, CALIFORNIA

January 31, 1965

Final Report

ELECTRICAL EFFECTS OF SHOCK WAVES: CONDUCTIVITY IN CsI, KI, AND NaCL.

Prepared for:

BALLISTIC RESEARCH LABORATORIES
ABERDEEN PROVING GROUND
MARYLAND

CONTRACT DA-04-200-ORD-1279

By: W. MURRI D. G. DORAN
POULTER RESEARCH LABORATORIES

SRI Project PGU-4100

Approved: D. L. BENEDICT, DIRECTOR
POULTER RESEARCH LABORATORIES

Copy No. 5

BLANK PAGES
IN THIS
DOCUMENT
WERE NOT
FILMED

ABSTRACT

The electrical resistivities of single crystal NaCl, KI, and CsI have been measured at several shock pressures in the range from 120 to 300 kbar. The resistivity of NaCl remained > 9×10^3 Ω-cm at 225 kbar. One shot in which the specimen was preheated to 480°C and shocked to 244 kbar gave an averaged resistivity of 470 Ω-cm. The resistivity of KI decreased to a value between 2 and 9 Ω-cm at 241 kbar; there is considerable scatter in the data below 190 kbar. Resistivity measurements on CsI were performed parallel and perpendicular to the direction of shock propagation; the resistivity decreased to 2 Ω-cm at 277 kbar in the first case and to ~0.2 Ω-cm in the latter. The data suggest a dependence of the conductivity on crystallographic direction. The data are consistent neither with electronic conduction caused by a decrease in the band gap due to shock compression of the lattice nor with ionic conduction caused by melting which may occur behind the shock front.

CONTENTS

CONTENTS

ILLUSTRATIONS

TABLES

I INTRODUCTION

In the past few years, many laboratories have studied the electrical effects associated with the propagation of shock waves in solids. Included in these effects are the depolarization of ferroelectric ceramics, the conductivity of sulfur and other materials, and the polarization of certain materials. The motivation for some of this work has been the search for explosive-sensitive and pressure-electric transducers.

Basic study of some of these phenomena should produce data and insight concerning the fundamentals of the shock process itself and should also provide tools for study of the changes induced in solids by shock waves. It is obvious, however, that a project of modest size must concentrate its efforts on a few specific areas of interest if it is not to be completely exploratory in nature. There is indeed considerable incentive for exploratory research—the need for diagnostic tools for pressure and temperature measurement, the need to avoid spurious electrical effects in present electrical measurements utilizing circuit elements which are shocked in the course of the measurement, and, of course, scientific curiosity.

In 1956, Alder and Christian reported some semiquantitative data on several ionic solids which indicated that their electrical conductivity dramatically increased when the solids were compressed by strong shock waves.[1] A study of this effect was begun two years ago (under BRL sponsorship)* at Stanford Research Institute[2] for the following reasons:

1. The effect was not predictable based on present knowledge.

2. Efforts by Griggs, *et al.*[3] and Drickamer[4] to detect the effect in static high-pressure apparatus were unsuccessful. The need for corroboration of the effect was heightened by the then-primitive state of electrical conductivity measurements in shock experiments.

3. If the effect were corroborated, it would be important to make the measurements more quantitative and to measure the pressure and temperature dependence of the conductivity so that the mechanism could be identified.

* A report covering the first year's work will be referred to herein as Report I. The contents of Report I will not be repeated here unless necessary for completeness.

4. The interpretation of the effect by Alder and Christian[1] as a metallic transition was not supported by the theoretical work of Flower and March.[5] Alternative interpretations needed to be examined.

During the period covered by Report I, the effect was corroborated, the measurements were made more quantitative, and a greater range of pressure and temperature was investigated. An alternative interpretation in terms of an ionic mechanism was suggested, but the mechanism was not positively identified.

II MATERIALS

The materials studied were NaCl, KI, and CsI; the major emphasis during 1964 has been on CsI.

The specimens of NaCl and KI were prepared from optical grade crystals obtained from Harshaw Chemical Co., Cleveland, Ohio. The NaCl specimens were single crystals. The KI specimens were poor single crystals in that they contained domains of slight misorientation ($\pm 1^\circ$ according to Harshaw). They were, however, easily cleavable. The KI and NaCl were cleaved to the desired thicknesses, which for the present experiments varied from 1 to 2-1/2 mm. Surface irregularities produced by cleaving were removed by lapping, so that final parallelism was within 0.001 inch. The KI crystals were kept desiccated until fired.

CsI crystals were obtained from Harshaw and from Isotopes Inc. The specimens from Harshaw, as noted in Report I, were polycrystalline with apparent domain size of the order of 1 mm; however, the crystals used in Shots 10,820 and 10,943 were single crystals obtained from Harshaw. The Isotope crystals were single crystal.

CsI crystals, not being cleavable, originally were cut either with a diamond saw or with a thin blade held stationary as the crystal rotated in a lathe. During the latter part of the work the CsI crystals were cut with a wire saw, and the surfaces lapped flat with 600 grit paper and alcohol.

All specimens were circular disks 25 mm in diameter except those used in the transverse geometry shots.

III EXPERIMENTAL TECHNIQUE

A. SHOT CONFIGURATION

The "longitudinal geometry" in which the direction of the current is parallel to the propagation direction of the shock is shown in Figure 1. The driver plate, which also served as one electrode, was 2024T aluminum for all shots. The backing electrode was aluminum for CsI specimens and magnesium for NaCl and KI specimens, in order to match approximately the shock impedances of specimen and electrode. This electrode was usually 22 mm in diameter; thus when no insulation was used the outer 1-1/2 mm of the upper surface of the crystal and the curved edge were free. For some shots, the sample was insulated laterally with Dow Corning silicone fluid No. 200 (electrical grade—200 cs).

The electrical leads were connected to the backing electrode at least 12 mm from the specimen, so that the shock would not reach the junction during the time of measurement ($\sim 1\,\mu$sec after shock transit). For the same reason, the ground leads were connected at the top of a 30-mm-high aluminum cylinder which rested on the driver plate. This also avoided a possible thermal emf which could be generated at the junction of the steel screw with the aluminum driver (see Report I, Part I) if the screw were used as a portion of the ground connection.

On each shot we included a pressure transducer of the resistance wire type (Manganin wire in C-7 epoxy).[6] This served not only to monitor the shock strength but also to provide an excellent time reference signal. The transducer signal and the specimen signals were displayed on the two beams of a Tektronix 551 oscilloscope for direct comparison. The gauge wire was 1 mm from the epoxy-driver plate interface, but shock arrival at the interface was indicated by a small polarization signal[7] and hence no correction for shock transit in the C-7 was necessary.*

* Some of the shots included a gauge of slightly different design from that developed and tested extensively in these laboratories. The altered design was intended to give greater time coverage—which it did. However, the indicated peak pressures were erratic and have been discounted. The records from these gauges were used only as a time reference.

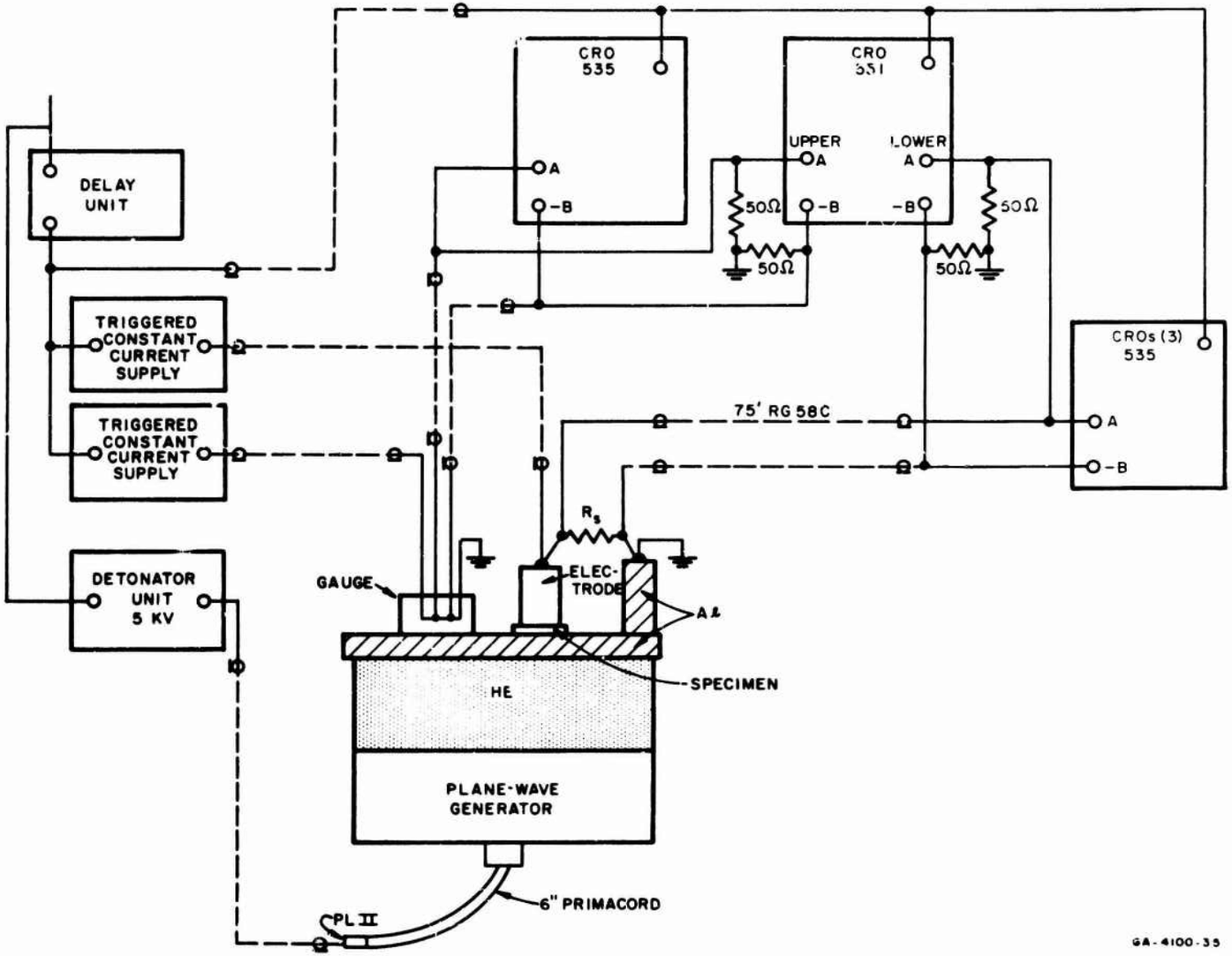

FIG. 1 SHOT CONFIGURATION FOR THE LONGITUDINAL GEOMETRY AND THE CONSTANT-CURRENT MEASURING CIRCUIT

A few shots were fired in which two specimens were studied simultaneously. These were experiments in which one specimen assembly served as a control for a parameter change in the other.

For the "transverse geometry" (Figure 2), the current direction is perpendicular to the direction of shock propagation. The sample was a nearly rectangular block, 6.35 × 4 × 25.4 mm, which was supported on all sides (but not the ends) by the same material as that of the sample. Teflon sheet, 0.003 inch thick, was used as electrical insulation. The electrodes were strips of 0.001-inch aluminum foil, 6.35 mm wide, placed equidistant from the ends of the sample (see Figure 2). A brass bar was fastened with epoxy to each of the side-supporting blocks and all electrical connections were made to these bars. The constant-current measuring circuit was used (see Section B below). The sample, supporting blocks, electrodes, and Teflon insulation were all assembled and held tightly with

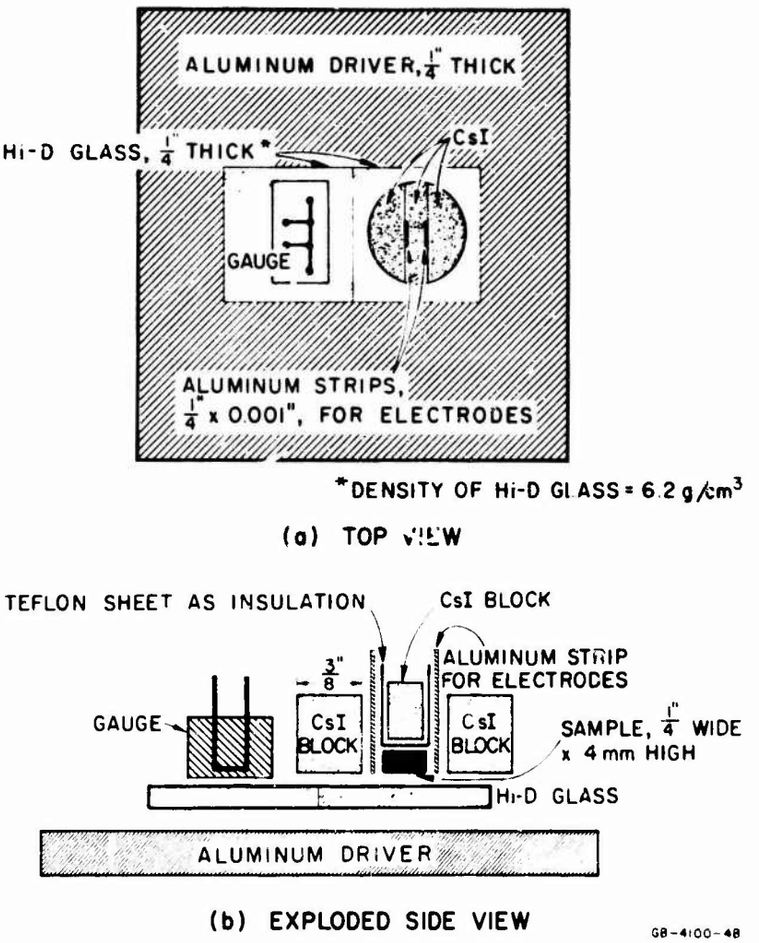

FIG. 2 SHOT CONFIGURATION FOR THE TRANSVERSE GEOMETRY

a clamp while the edges were cemented with epoxy. This sample assembly was insulated electrically from the aluminum driver by a 1/4-inch-thick plate of Hi-D glass (density 6.2 g/cm^3).* A Manganin-wire pressure transducer of the kind described earlier was mounted on a similar glass plate.

The transverse geometry technique allows a measurement of the sample resistance as a function of time during shock passage through the sample and for about 1 μsec after shock exit from the sample. After this time, relief waves from the edges reach the electrodes and the measurement is no longer accurate.

B. METHOD OF MEASUREMENT

In the work of Report I we used a "constant-voltage" circuit. For the shots this past year the "constant-current" system shown in Figure 1 was used almost exclusively.

In this system, the power supply and oscilloscope sweep are triggered 5 μsec before the shock reaches the specimen. An additional 1-μsec delay in the power supply permits display of a portion of the baseline. Hence the voltage drop across the shunt resistor is measured during the early portion of the sweep (the specimen resistance being effectively infinite) and the voltage drop across the shunt resistor and shocked specimen in parallel is measured during the latter portion of the sweep. An effectively constant current is obtained because the power supply time constant is many hundreds of microseconds and the ballast resistance is at least fifty times the shunt resistance.

When this system was first used, it was found necessary to use a differential preamplifier at the oscilloscope for shunt resistances $< 1\ \Omega$; that is, separate signal leads detected the voltage with respect to ground at each end of the shunt, and the difference between the signals was displayed on the oscilloscope. Even using this system, we found that the signal level prior to shock arrival might drift slightly (usually decreasing in magnitude) for a shunt resistance of 0.02 Ω, which seems to indicate that some contact resistance was varying with time. Since the effect seems to be unpredictable, this resistance may depend on such factors as the quality of the solder contacts, although preliminary checks indicate

* From other work in this laboratory, the resistivity of this material under shock compression is known to remain high at the pressures of interest.

negligible contact resistance. The maximum current used is 10 amp, which should cause negligible heating of the resistors in the circuit for the short time of interest ($\sim 10\,\mu$sec).

It was found later that the differential system was unnecessary if a ground loop through the constant current power supply was avoided. This was accomplished by isolating the chassis from the common ground of the 3-wire 110-volt power and from the delay unit by means of a pulse transformer at the trigger input.

The sample resistance R_x is determined from the shunt resistance R_s, the signal prior to shock arrival V_0, and the final signal V (measured within $\sim 0.5\,\mu$sec after the shock leaves the specimen):

$$R_x = R_s[(V_0/V) - 1]^{-1} \qquad (1)$$

An example of the type of record obtained is shown in Figure 3. A constant-current system is used with a gauge; a shunt resistor is not required, of course, because the initial resistance is finite. The Manganin resistance increases with pressure so that the signal amplitude increases when the shock reaches the wire. A small polarization signal can be seen when the shock first enters the insulating material (C-7 epoxy) of the gauge.

C. SUBMICROSECOND MEASUREMENT OF LOW RESISTANCE

To gain a better understanding of the behavior of the circuitry, several small-scale shots were fired with various electrode configurations, shunt resistance and inductance, and ways of handling electrical grounds.

Experiments in which the shunt resistance was shorted produced signals which initially dropped very rapidly, then much more slowly, toward the baseline (see Figure 4). Several microseconds were required before a short was indicated. The slow decay is consistent with the measured $\sim 0.1\,\mu$H inductance of the circuit. The initial drop is not yet understood, but circuit inductance seems to be a limiting factor in measurements of low resistance.

The time constant is decreased by increasing the shunt resistance R_s; for a given R_x, this means decreasing V (see Eq. 1). Since maximum accuracy is not required, we can sacrifice the display of V_0 and increase

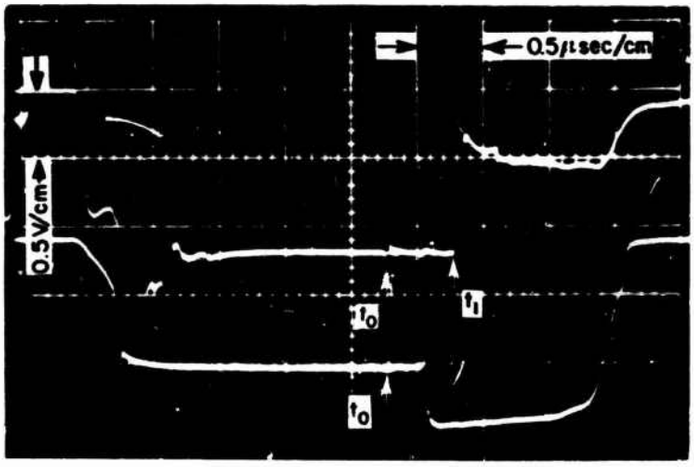

(a) RECORD FOR SHOT NO. 10,313
UPPER BEAM—CONDUCTION SIGNAL
LOWER BEAM—GAUGE SIGNAL

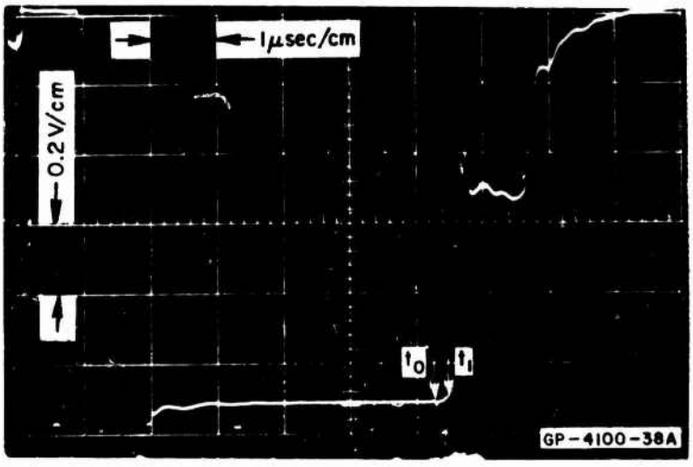

(b) RECORD FOR SHOT NO. 10,102
CsI, Rs = 0.1 Ω

FIG. 3 TYPICAL OSCILLOSCOPE RECORDS FROM CONDUCTION SHOTS (t_0 and t_1 correspond to the shock entering and exiting the sample respectively.)

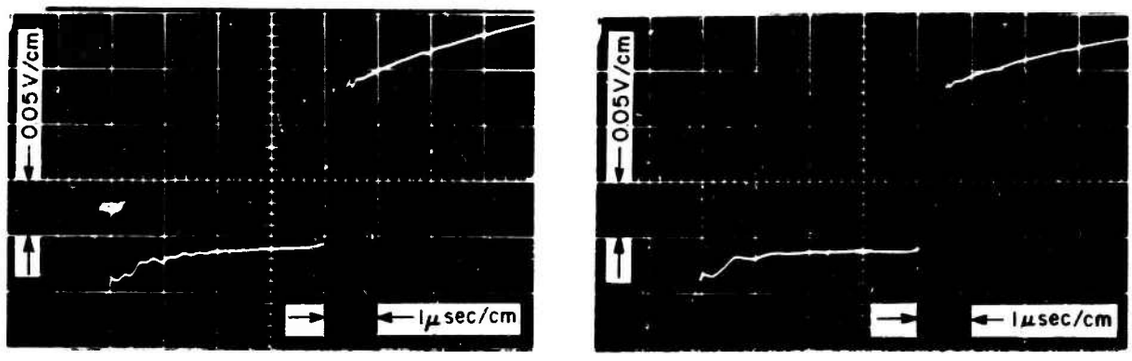

(a) SHOT NO. 10,090 —— 0.02Ω SHUNT

(b) SHOT NO. 10,091 —— 0.02Ω SHUNT

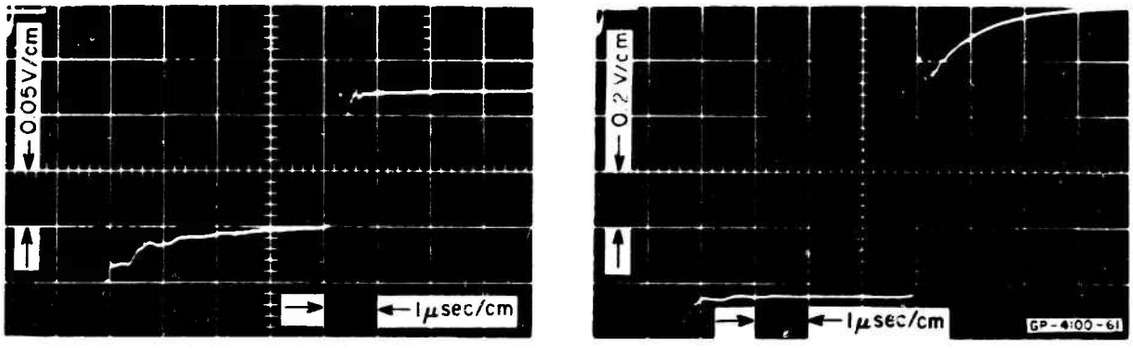

(c) SHOT NO. 10,092 —— 0.02Ω SHUNT AND 0.02Ω IN SERIES WITH ELECTRODE

(d) SHOT NO. 10,093 —— 0.1Ω SHUNT

FIG. 4 OSCILLOSCOPE RECORDS FROM SHORTING SHOTS

oscilloscope sensitivity in order to study V. A Zener diode was used to clip the signal in order to avoid overdriving the oscilloscope, but its rise time was too long. The diode was found to be unnecessary, however, for reasonable R_s values.

Another approach to the measurement of small resistances was to return to the constant-voltage circuit described in Report I. For this circuit

$$R_x = R_s[(V_0/V) - 1] \qquad (2)$$

and small values of R_x/R_s mean $V \simeq V_0$. A Tektronix Z-type preamplifier was used to expand the small difference between V and V_0. The requirement of constant voltage is more stringent when the type Z preamplifier is used, and the time constant was consequently increased by increasing the

capacitance. It was necessary to place a number of 2-μf capacitors in parallel* to achieve the desired value, and the inductance was thereby increased. No improvement over the constant-current circuit was achieved.

D. PREHEATED SPECIMENS (HOT SHOTS)

The design of the hot shots (indicated in Figure 5) was based on a desire to preheat the crystal specimens to $\sim$500°C prior to firing in a configuration as close as possible to that used for room temperature shots. It was found possible to do this without remote handling of the explosive.

Both electrodes were heated externally by resistance wire; the temperature of each was monitored with a separate thermocouple. The bottom electrode (1/4-inch thick) was insulated from the remainder of the driver plate (1/4-inch thick) by a 9-mil air gap. A Manganin wire gauge rested on a similar assembly. The aluminum surfaces were polished to reduce heat transfer and the periphery of the driver plate was water-cooled; nevertheless, the temperature at the center of the driver plate exceeded somewhat the softening temperature of the explosive. The explosive temperature was reduced to an acceptable level by a sheet of 9-mil Mylar between aluminum driver and explosive. The heating time to 480°C was about 20 minutes.

Detailed calculations of shocked states in preheated specimens are presented in Appendix A.

---

* Paper capacitors have been found best for rapid release of energy; none larger than 2 μf was readily available.

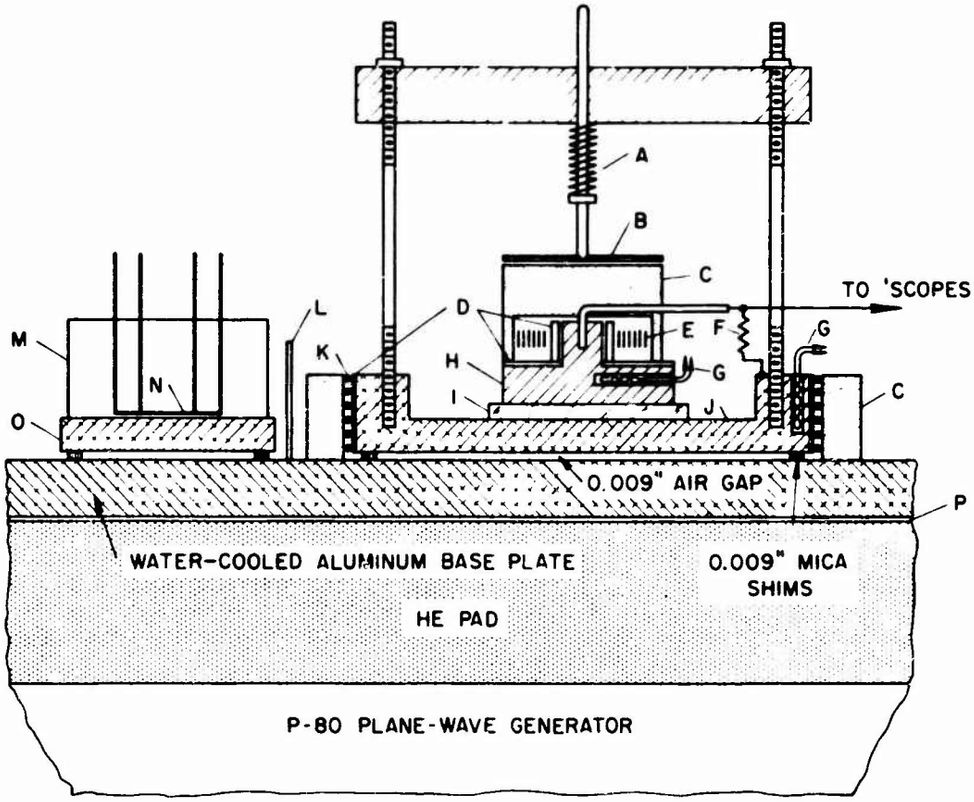

A	SPRING	I	CRYSTAL
B	TOP HEATER ASSEMBLY	J	ALUMINUM BOTTOM ELECTRODE
C	ASBESTOS	K	BOTTOM HEATER WINDINGS
D	QUARTZ AND MICA INSULATION	L	THERMAL SHIELD
E	HEATER WINDINGS	M	C-7 EPOXY
F	SHUNT RESISTOR	N	RESISTANCE WIRE PRESSURE GAUGE
G	THERMOCOUPLES	O	ALUMINUM
H	TOP ELECTRODE	P	MYLAR

GB-4100-44

FIG. 5 SCHEMATIC DIAGRAM OF HOT SHOT ASSEMBLY

IV EXPERIMENTAL RESULTS

All conductivity shots fired during this report period are included in Table I. Except for Shots 10,941 and 10,942, all measurements were made with the constant-current system.

The resistivity data from all shots are plotted *vs.* pressure in Figures 6 and 7, *vs.* volume in Figures 8 and 9, and *vs.* $1/T$ in Figures 10, 11, and 12. (The errors due to the uncertainties in interpreting the oscilloscope records are discussed in Section V.) For the longitudinal geometry, the measured resistance has been converted to resistivity using the compressed specimen thickness and the upper electrode area.

The resistivity of NaCl shocked to 225 kbar from room temperature was determined to be $> 9 \times 10^3$ Ω-cm. The only shot for which appreciable conductivity was observed in NaCl was Shot No. 10,504, in which the NaCl was heated to 480°C and then shocked to 244 kbar. The resulting resistivity was between 186 and 753 Ω-cm.

The resistivity of KI decreases to a value of about 6 Ω-cm at a pressure of 240 kbar; a leveling off is indicated by both the pressure and volume plots (Figures 6 and 8). Shot No. 10,939 at 120 kbar produced a resistivity of 27 Ω-cm, which is lower than other results. The records from this shot do not show any anomalies, however, and it has therefore not been discarded. The initial temperature of all shots was about 25°C.

For CsI in the longitudinal geometry, the resistivity decreases from $\sim 10^5$ Ω-cm at 122 kbar to ~6 Ω-cm at 250 kbar. As in the case of KI, a leveling off at high pressure is indicated in Figures 7 and 9.

It should be noted that the longitudinal geometry, constant-voltage data from Report I do not agree with the longitudinal data obtained in the present work with the constant-current circuit for resistivities > 15 Ω-cm. For this reason, two constant-voltage longitudinal shots (Nos. 10,941 and 10,942) were fired in the present work. The results agree well with the present constant-current longitudinal data, leaving a very large discrepancy between data in this report and those in Report I.

Table I

SHOT PARAMETERS AND RESISTIVITY DATA FOR ROOM

SHOT NO.	CRYSTAL		ELECTRODE DIAMETER (in.)[a]	SHUNT RESISTANCE (Ω)	LATERAL INSULATION[b]	HIGH EXPLOSIVE[c]	DRIVER MATERIAL AND THICKNESS	STATE	
	Type	Thickness (mm)						Stress (kbar)	Spec Vol (cm
9,994	NaCl	2.38	5/8	25.5	Oil	2"Comp B-3	1/2" Al[e]	200	0.3
10,101		1.01	7/8	0.02	Air			210	0.3
10,306[f]		2.18	7/8	0.21	Air			205	0.3
10,312	[g]	2.06	7/8	0.20	Air			205	0.3
9,997		2.84	5/8	25.5	Oil	2" 9404		225	0.3
10,504	[h]	2.385	7/8	25.5	Air	4" 9404		244	0.3
10,939	KI	1.777	7/8	25.5	Air	1/2" Comp B-3 +1" Baratol	1/2" Al	121	0.2
10,936		1.777	7/8	25.5	Air	2" TNT	1/2" Al	155	0.2
9,998		1.786	5/8	25.5	Oil	2" Comp B-3	1" Al	190	0.1
10,099		1,013	7/8	0.02	Air		1/2" Al	205	0.1
10,094		1.834	5/8	0.02	Air			206	0.1
10,001		1.820	5/8	0.02	Oil			207	0.1
10,311	[g]	2.03	7/8	0.20	Air			206	0.1
10,098		0.988	7/8	0.108	Air			214	0.1
10,103		1.105	7/8	0.106	Air	2" 9404		242	0.1
10,314[f]		2.30	7/8	3.31	Air	2" 9404		237	0.1
10,929	CsI	1.777	7/8	25.5	Oil	2" Baratol	1/2" Al	122	0.1
10,930		1.777	7/8	25.5	Oil	1/2" Comp B-3 +1" Baratol	1/2" Al	154	0.1
10,822		1.676	7/8	25.5	Air	1/2" Comp B-3 +1" Baratol	1/2" Al	151	0.1
10,821		1.83	7/8	25.5	Air	2" TNT	1" Al	187	0.1
10,820		1.74	7/8	25.5	Air	2" TNT	1/2" Al	206	0.1
9,995		1.70	5/8	25.5	Oil	2" Comp B-3	1" Al	230	0.1
9,999		2.435	5/8	0.02	Oil		1/2" Al	241	0.1
10,097		0.981	7/8	0.103	Air			256	0.1
10,306[f]		1.77	7/8	0.17				251[i]	0.1
10,307		1.51	7/8[j]	0.19				253[i]	0.1
		1.68	7/8[j]	0.23				252[i]	0.1
10,308		1.28	7/8	0.17				254[i]	0.1
		1.29	7/8	0.17				254[i]	0.1
10.315		2.54	1/4[k]	3.40				247[i]	0.1
		2.54	7/8	0.20				247[i]	0.1
10,096		1.008	7/8	0.85				262	0.1
10,309		2.34	1/4[k]	3.40		2" 9404		277[i]	0.1
		2.34	7/8	0.20				277[i]	0.1
10,310	[g]	2.49	7/8	0.21				276[i]	0.1
		2.54	7/8	0.18				276[i]	0.1
10,313	[g]	2.49	7/8	0.20				276[i]	0.1
10,314[f]		2.44	7/8	3.43				276[i]	0.1
10,102		1.023	7/8	0.116				298	0.1
10,100		1.780	7/8	0.110			3/8" Al	(475)[j]	--
10,503	[h]	2.005	7/8	0.195		2" TNT	1/2" Al	181	0.1
10,931	[h]	1.777	7/8	0.265		2" Comp B-3	1" Al	230	0.1
10,932	[h]	1.777	7/8	0.273		2" Comp B-3	1" Al	232	0.1
10,943		[l]	[l]	30.0		1/2" Comp B-3 +1" Baratol	1/2" Al +1/4" Hi-D	118	0.1
10,940		[l]	[l]	42.8		2" TNT	1/2" Al +1/4" Hi-D	144	0.1
10,934		[l]	[l]	0.91		2" Comp B-3	1/2" Al +1/4" Hi-D	203	0.1
10,937		[l]	[l]	1.07		2" 9404	1/2" Al +1/4" Hi-D	255	0.1
10,942		1.777	7/8	25.5	Air	2" Baratol	1/2" Al	129	0.1
10,941		1.777	7/8	25.5	Air	2" TNT	1/2" Al	169	0.1

Notes:

[a] Mg for NaCl and KI; Al for CsI.

[b] Oil was Dow Corning 200 fluid; viscosity = 200 cs.

[c] Initiated by a P-60, 6-inch plane-wave generator, except preheated shots for which P-80 planewave generator was used.

[d] Average state at time of measurement; see Table III.

[e] 2024T Al.

[f] One-half of double shot.

[g] Irradiated 90 hours with Co^{60} γ-rays; 2 x

[h] Crystal preheated.

[i] Shock stress estimated.

[j] See Sec. IV B.

[k] See Sec. IV A.

[l] Transverse sample 1/4 x 1/4 x 0.16 in.;

Table I

ISTIVITY DATA FOR ROOM TEMPERATURE AND HOT SHOTS

DRIVER ERIAL AND ICKNESS	STATE IN SPECIMEN[d]			RESISTIVITY (Ω-cm)	REMARKS
	Stress (kbar)	Specific Volume (cm^3/g)	Temperature (^oK)		
/2" Al[e]	200	0.330	1073	$> 5 \times 10^4$	
	210	0.3275	1105	---	
	205	0.3285	1105	> 600	
	205	0.3285	1105	∞	Fired 27 hours after 2×10^7 rad exposure.
	225	0.323	1134	$> 0.9 \times 10^4$	
	244	0.326	2340	753 - 186	Crystal preheated to 480°C.
/2" Al	121	0.2109	1645	28	
/2" Al	155	0.2015	2325	131	
1" Al	190	0.1940	2971	116^{+8}_{-4}	
/2" Al	205	0.1915	3440	---	
	206	0.1910	3550	---	
	207	0.1908	3560	---	
	206	0.1913	3540	8 - 20	Fired 25 hours after 2×10^7 rad exposure.
	214	0.1897	3640	10 ± 5	
	242	0.1848	4500	9^{+0}_{-7}	
	237	0.1855	4540	2 - 7	
/2" Al	122	0.1526	1450	$\gtrsim 1.6 \times 10^4$	
/2" Al	154	0.1484	2030	612	
/2" Al	151	0.1488	2075	160	
1" Al	187	0.1444	2665	29	
/2" Al	206	0.1423	2970	22	
1" Al	230	0.1395	3460	12 ± 3	
/2" Al	241	0.1382	4110	---	
	256	0.1366	4260	5.3^{+0}_{-2}	
	251[i]	0.1371	4240	1 - 20	
	253[i]	0.1370	4240	2 - 8	Electrodes coated with silver.
	252[i]	0.1371	4240	4 - 14	
	254[i]	0.1368	4250	2 - 6	Electrodes coated with graphite.
	254[i]	0.1368	4250	3 - 20	
	247[i]	0.1377	4220	1.7 - 4.2	1/4" electrode inside 7/8" OD guard ring.
	247[i]	0.1377	4220	3.3 - 6.7	
	262	0.1361	4375	5.1 ± 1	
	277[i]	0.1344	5210	3 - 3.3	1/4" electrode inside 7/8" OD guard ring.
	277[i]	0.1344	5210	1.2 - 1.6	
	276[i]	0.1345	5200	---	Fired 7 hours after 2×10^7 rad exposure. Trace appears normal for 0.4 μsec, then goes rapidly across base line.
	276[i]	0.1345	5200	---	
	276[i]	0.1345	5200	2.7 - 4.2	Fired 30 hours after 2×10^7 rad exposure.
	276[i]	0.1345	5200	4	
	298	0.1325	5600	6.8^{+1}_{-3}	
3/8" Al	(475)[j]	---	----	(< 0.8)	Flying plate shot.
/2" Al	181	0.1482	3620	1.78	Crystal preheated to 420°C.
1" Al	230	0.1400	3780	$\lesssim 0.3$	Crystal preheated to 100°C.
1" Al	232	0.1419	4540	$\lesssim 0.3$	Crystal preheated to 350°C.
/2" Al /4" Hi-D	118	0.1530	1425	19	Shot fired in transverse geometry.
/2" Al /4" Hi-D	144	0.1496	1820	(0.2)	Shot fired in transverse geometry.
/2" Al /4" Hi-D	203	0.1425	2965	0.61 - 1.3	Shot fired in transverse geometry.
/2" Al /4" Hi-D	255	0.1368	3965	0.18	Shot fired in transverse geometry.
/2" Al	129	0.1515	1575	2.3×10^5	Constant voltage.
/2" Al	169	0.1465	2390	46	Constant voltage.

90 hours with Co^{60} γ-rays; 2×10^7 rad dose.

heated.

s estimated.

B.

A.

sample 1/4 x 1/4 x 0.16 in.; electrode width 1/4 in.

B

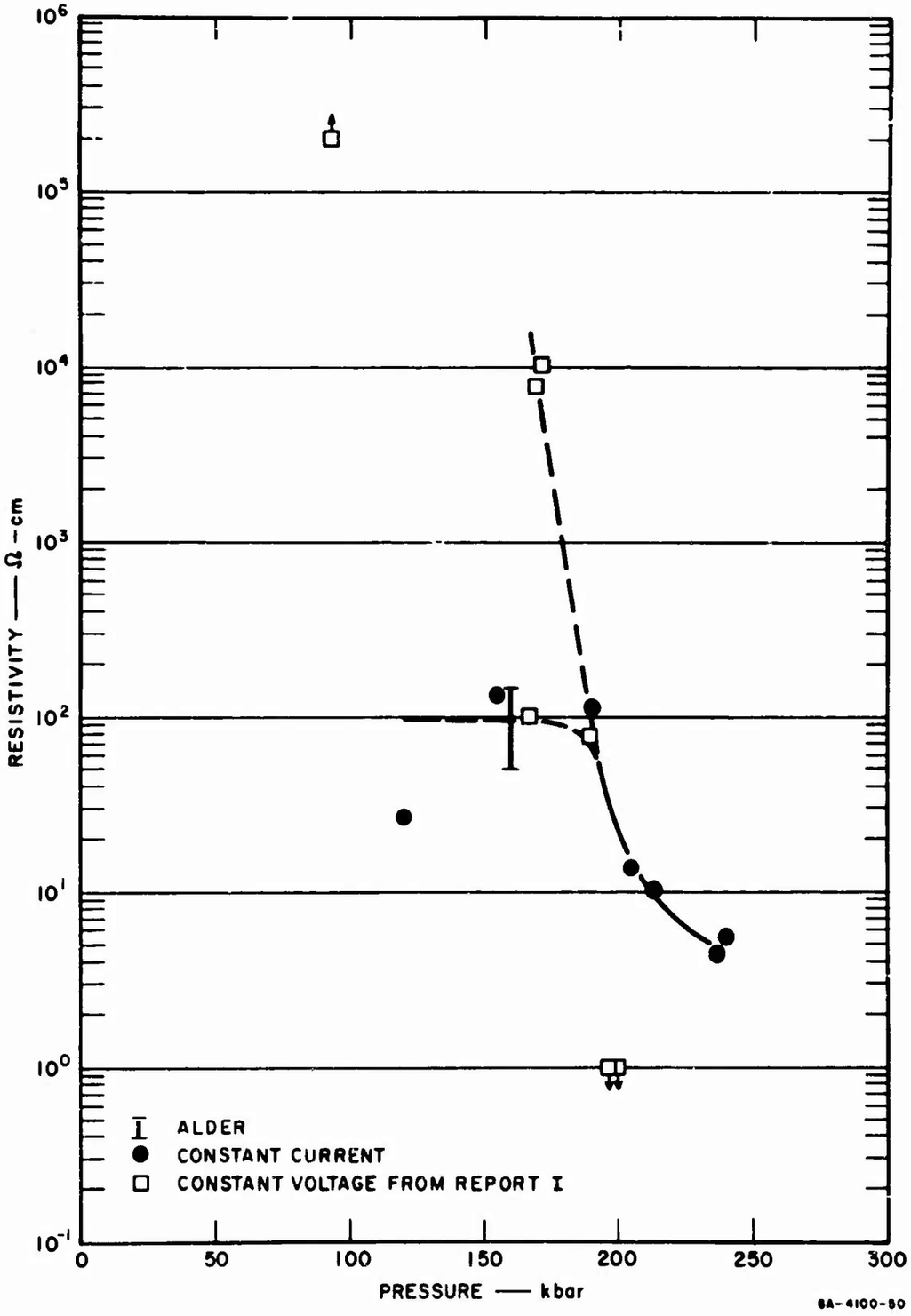

FIG. 6 RESISTIVITY vs. PRESSURE FOR KI. POINTS WITH ARROWS INDICATE LIMITS.

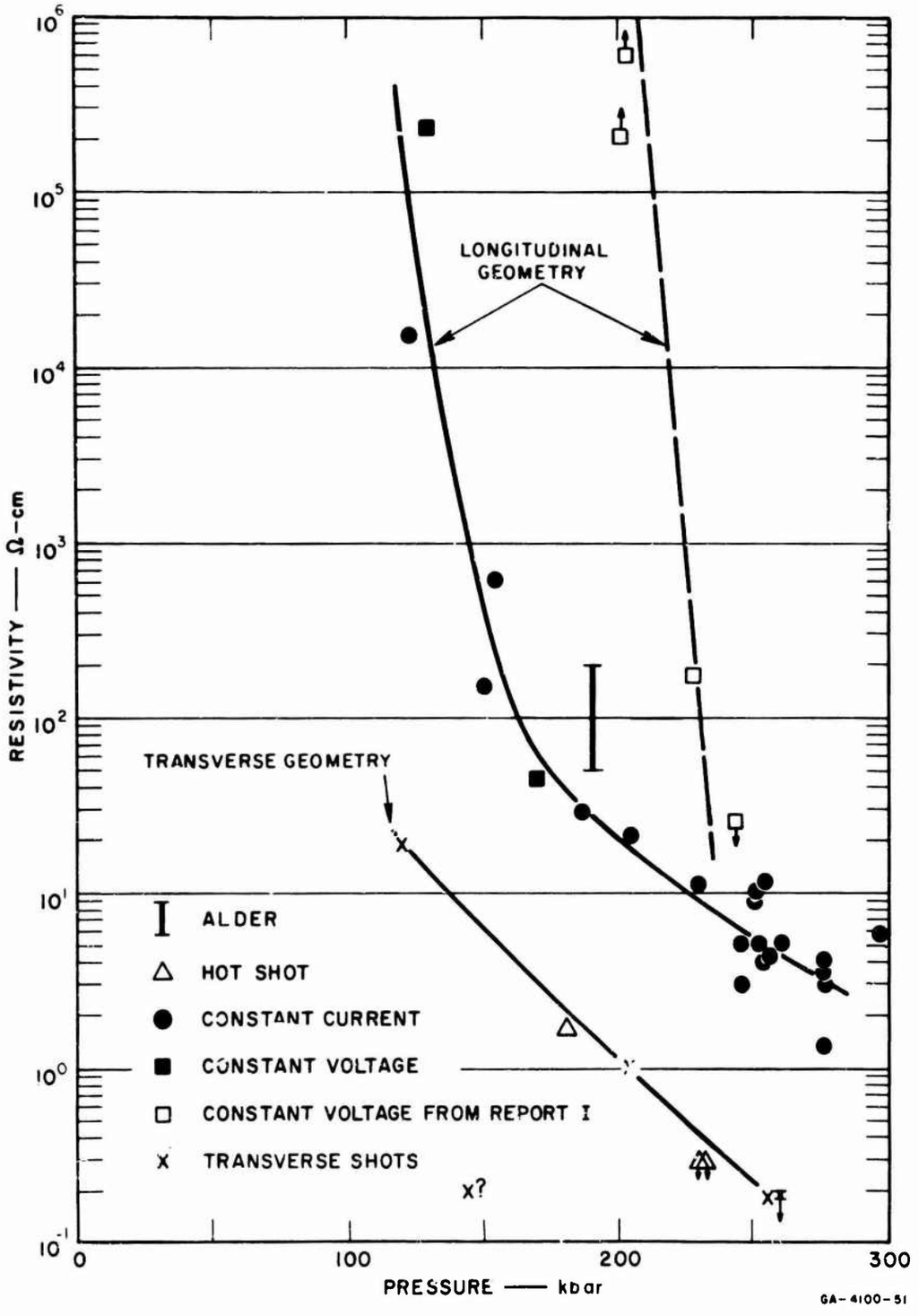

FIG. 7 RESISTIVITY vs. PRESSURE FOR CsI. POINTS WITH ARROWS INDICATE LIMITS. (Longitudinal shots with resistivity > 15 Ω-cm and all transverse shots were Harshaw single crystals shocked in the <III> direction.)

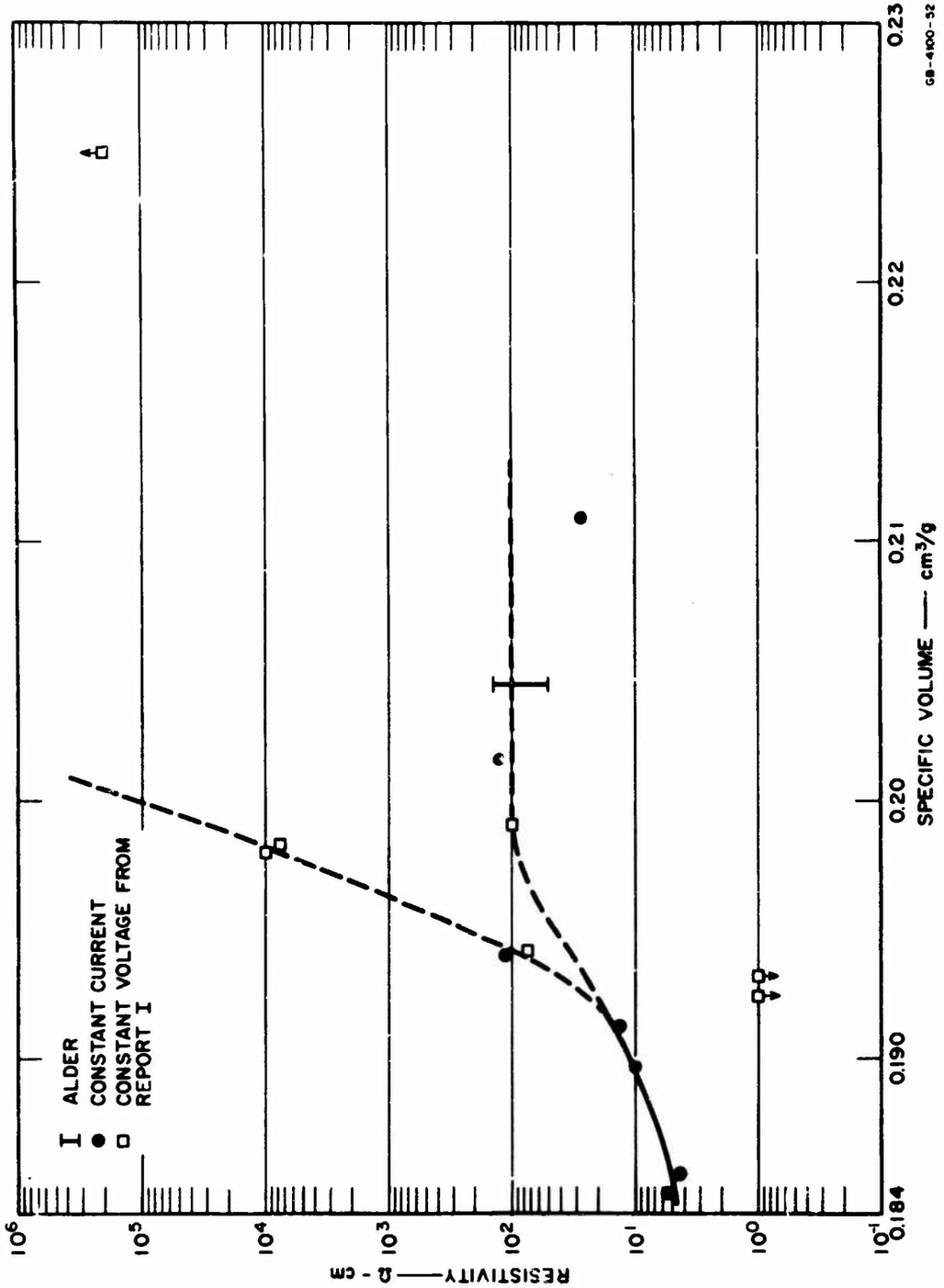

FIG. 8 RESISTIVITY vs. SPECIFIC VOLUME FOR KI. POINTS WITH ARROWS INDICATE LIMITS.

FIG. 10 RESISTIVITY vs. 1/T FOR NaCl. POINTS WITH ARROWS INDICATE LIMITS.

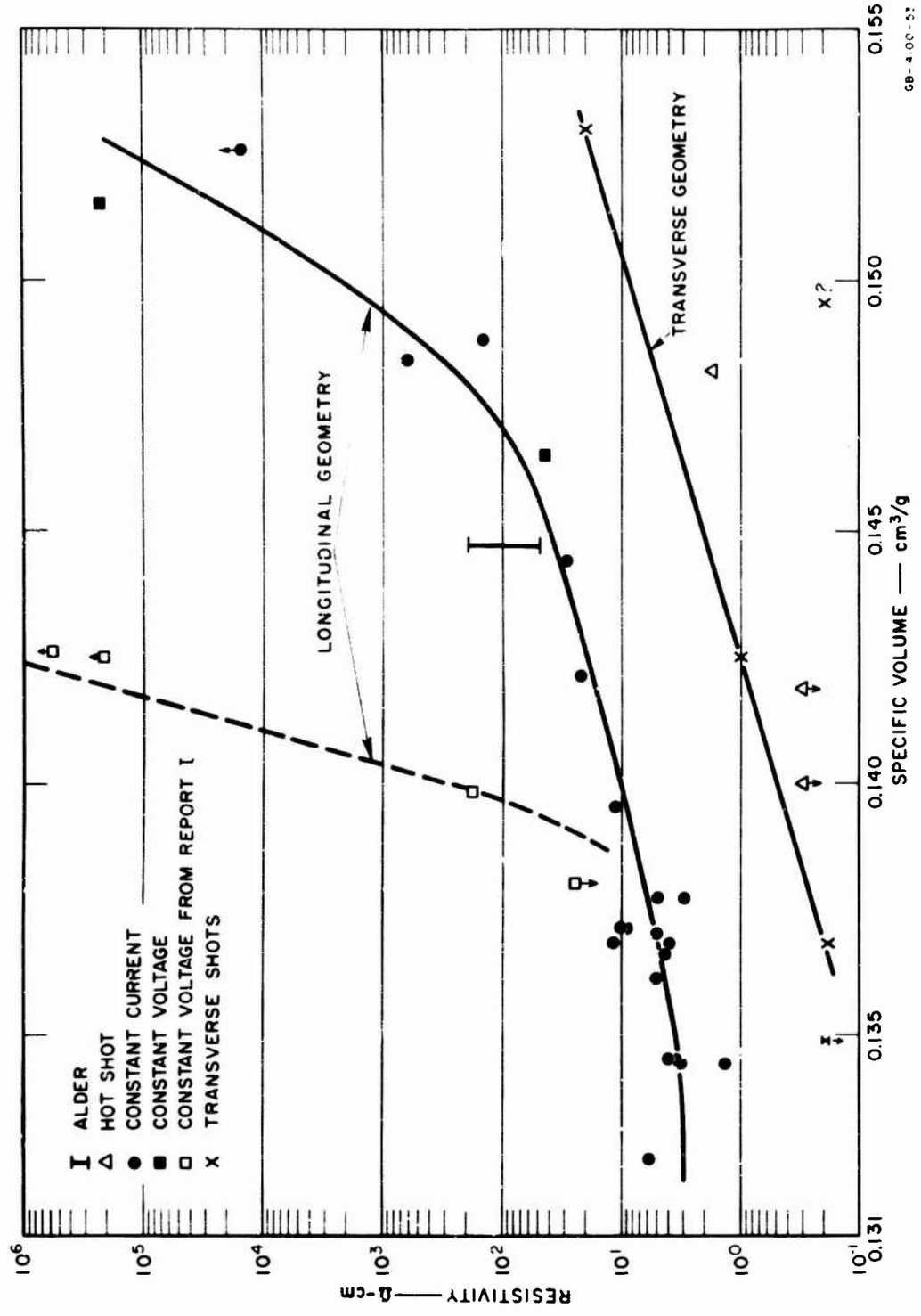

FIG. 9 RESISTIVITY vs. SPECIFIC VOLUME FOR CsI. POINTS WITH ARROWS INDICATE LIMITS.
(See caption in Fig. 7)

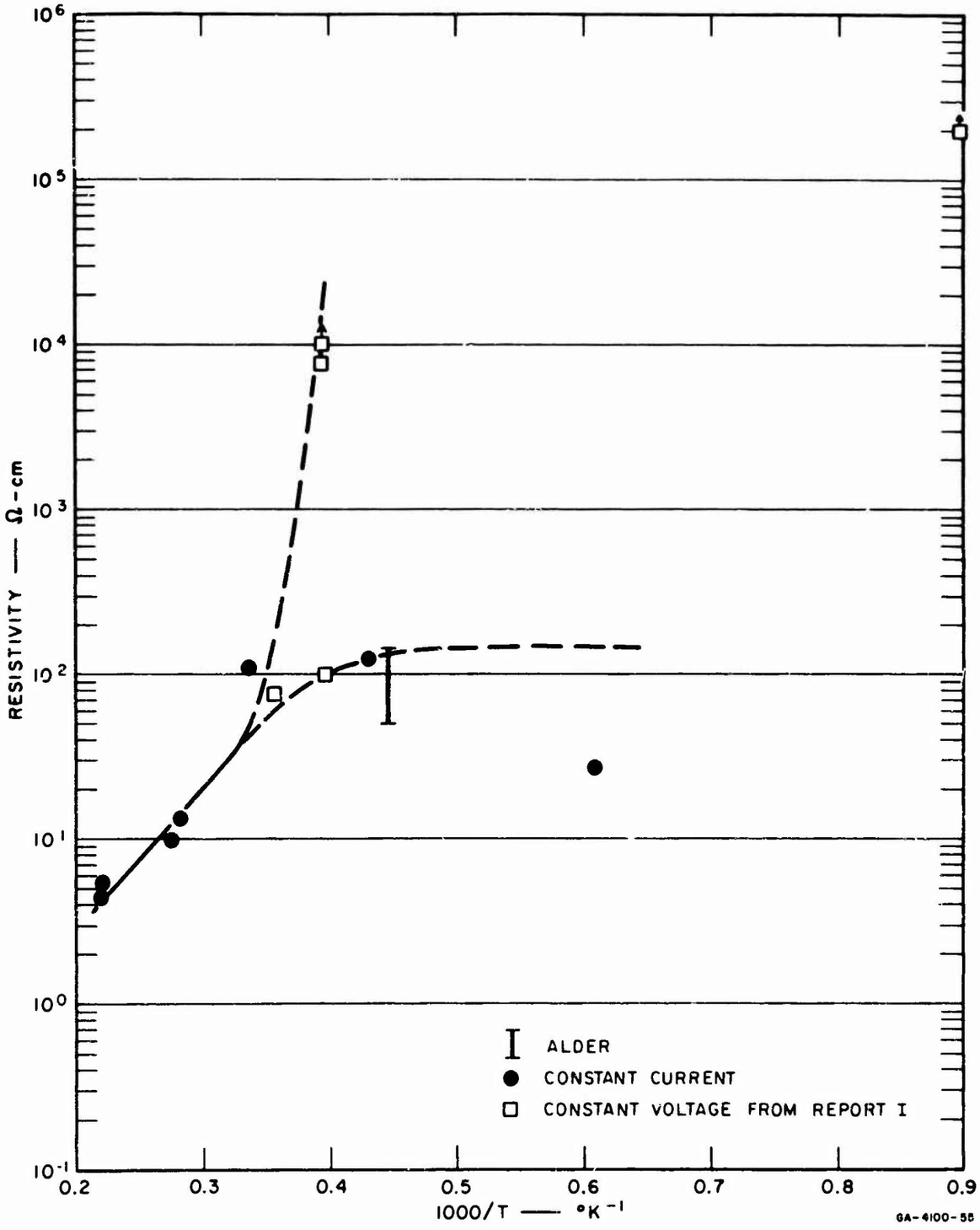

FIG. 11 RESISTIVITY vs. 1/T FOR KI. POINTS WITH ARROWS INDICATE LIMITS.

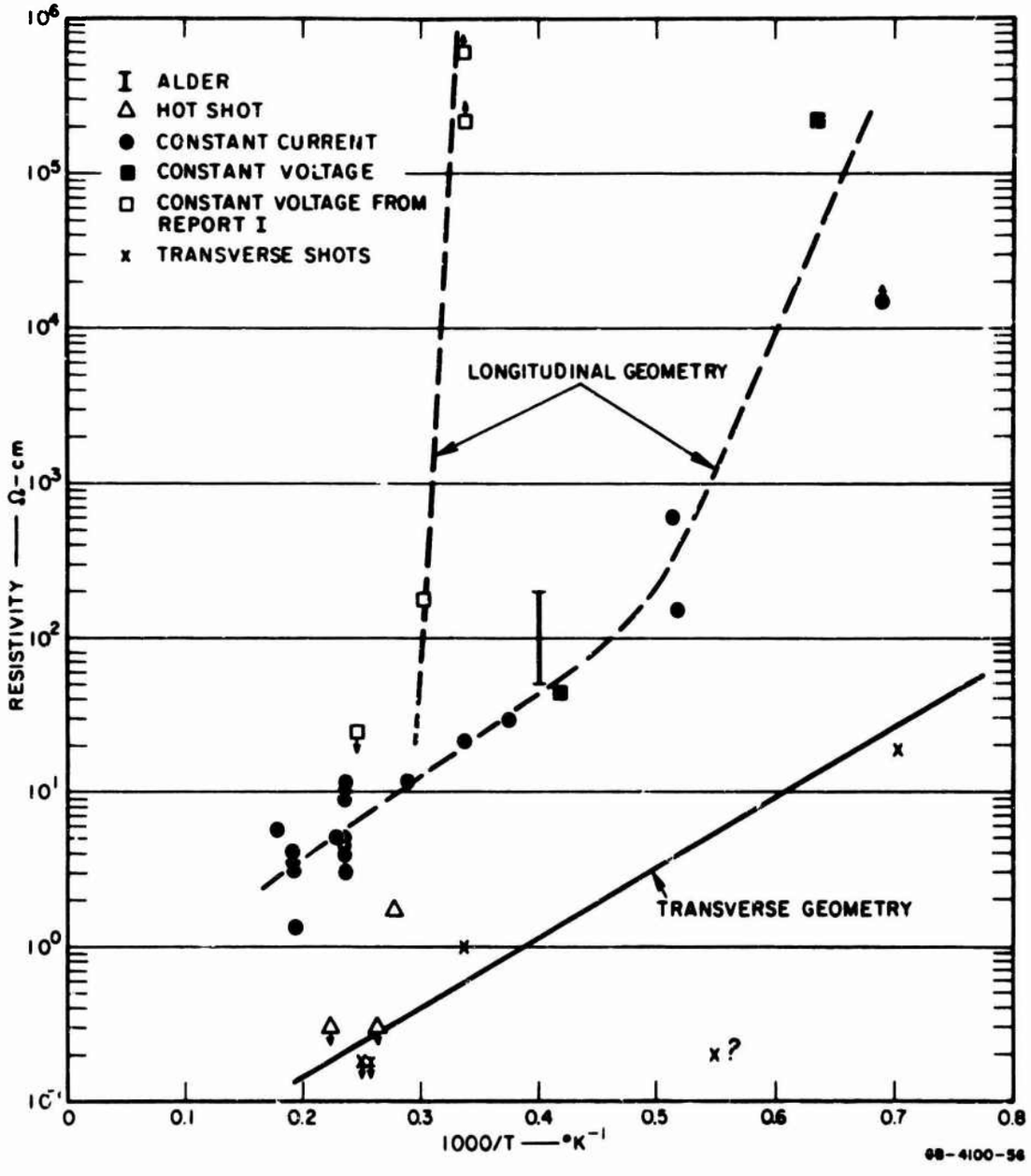

FIG. 12 RESISTIVITY vs. 1/T FOR CsI. POINTS WITH ARROWS INDICATE LIMITS. (See caption in Fig. 7)

The CsI specimens used during this report period were of three types. (1) Harshaw, nominally polycrystalline; (2) Harshaw single crystals; and (3) Isotope single crystals. The specimens from which the data of Report I were derived were of type (1). The present data for resistivities > 15 Ω-cm in longitudinal geometry and for all transverse shots were obtained with type (2) crystals shocked in the <111> direction. Thus the discrepancy may be due to a dependence on crystallographic orientation and/or impurity content.

In the transverse geometry, the resistivities are lower than for the longitudinal geometry,* decreasing to 0.2 Ω-cm at 255 kbar. Measurements in the two geometries differ in two respects, viz., the direction of current flow relative (1) to the crystal orientation and (2) to the direction of shock propagation. The direction of current flow in the transverse shots was perpendicular to the <111> direction but otherwise random. In view of this and of a similar effect found in KI shocked in the <100> direction (see Report I), a dependence of resistivity on direction of current flow relative to the shock direction seems most likely.

Several shots were fired in which the experimental parameters were varied. The results of these shots and the parameters varied are described in the following subsections.

A. VARIATION OF ELECTRODE AREA

For Shot No. 10,315, the backing electrode was divided into a central 0.250-inch-diameter electrode surrounded by a 0.875-inch-OD × 0.270-inch-ID guard ring; the 0.010-inch annulus was filled with Teflon. The shunt resistances across the electrode and guard ring were made inversely proportional, and the currents through each directly proportional, to their respective areas. This was to provide a uniform current density in the specimen (to the extent that the resistivity was uniform). The advantages of this geometry are that it eliminates any edge effect due to stress relief at the unsupported edge of the specimen, and it raises the resistance to be measured by decreasing the effective specimen area. The latter makes possible a large shunt resistance which should improve the time response of the system. Included in this shot were a second crystal with a solid backing electrode, and a pressure gauge. Shot No. 10,309 was identical except that it was fired with 9404 rather than Comp B.

---

* This result apparently conflicts with the work of Alder and Christian—see Section V-B.

The data of Table I show that the electrode with a guard ring gave essentially the same resistivity as a solid one, even though the actual resistances differed by an order of magnitude. The additional 40 to 50 kbar provided by 9404 compared with Comp B causes no appreciable change in resistivity. It is worth noting that the system using the electrode plus guard ring should be capable of indicating resistivity a factor of 10 lower than that observed.

B. VARIATION OF ELECTRODE MATERIAL

Shot No. 10,307 was fired for the purpose of comparing the resistivity of CsI as measured by using the usual aluminum electrodes with that measured by using electrodes coated with silver paint. The shot assembly consisted of two crystals, one with regular electrodes and one with coated electrodes, plus a pressure gauge. Shot No. 10,308 was identical, but the coating was graphite. The results are included in Table I. The coated and bare electrodes on a given shot produced records which were a little different from one another, but these differences were no greater than those observed in other bare electric shots. The resistivities were essentially the same for all four crystals.

C. VARIATION OF SHUNT RESISTANCE

To decrease the time constant due to circuit inductance, the shunt resistance for Shot No. 10,314 was raised to 3.4 Ω, about 10 times the expected specimen resistance. Several oscilloscopes were run at relatively high sensitivity so that the signal after shock transit could be measured, although the initial signal due to the shunt resistor was off scale. The initial signal was observed on another oscilloscope as a check on the current and shunt resistance. Again the resistivity was several Ω-cm although a value as low as several tenths Ω-cm should have been measurable.

D. IRRADIATED SPECIMENS

Shots were fired with crystals of NaCl, KI, and CsI which had been irradiated with Co^{60} γ-rays ($\sim 2 \times 10^7$ rad). There appears to be no significant change in the resistivity of NaCl or KI, but the polarization signal in NaCl is modified somewhat. On the other hand, either irradiation of CsI produced a very large effect (of a peculiar nature) or the shot was completely spurious for some unknown and unexpected reason.

E. PASSIVE SHOTS (NO APPLIED FIELD)

In the work described in Report I, several passive shots were fired with a constant-voltage circuit, and signals were observed in every case (CsI, KI, and NaCl). The nature of the signal varied greatly with specimen resistivity. It sometimes continued after the shock exited from the specimen, although the signal level was small compared with the conductivity signals and was ignored.

In the present work it was important to interpret correctly small conduction signals; therefore, several passive shots were fired (all with CsI). The passive shots are listed in Table II and a typical signal is shown in Figure 13(a). The record from an active shot is shown in Figure 13(b) for comparison. Note that there is a small "polarization signal" as the shock traverses the specimen and that it continues beyond the shock exit time t_1—typically for 1 to 2 μsec. The shots of Figure 13 were made with a guard ring electrode assembly. It is interesting that, for both shots, the signal from the center electrode exhibits more structure than does that from the guard ring.

Table II

PASSIVE SHOT DATA FOR CsI

SHOT NO.	SAMPLE THICKNESS (mm)	ELECTRODE AREA (cm^2)	SHUNT RESISTANCE (Ω)	PEAK PRESSURE (kbar)	MAXIMUM SIGNAL VOLTAGE[a] (volts)	DURATION OF SIGNAL AFTER SHOCK EXIT (μsec)
10,502	2.06	3.88	0.197	303	+0.26, −0.34	1.6
10,817	1.75	3.88	0.27	275	+0.30, −0.55	1.6
10,818	1.55	3.88	0.02	274	+0.22, −0.13	1.6
10,935[b]	1.77	0.316	3.51	266	+0.47, −0.33	1.4
	1.77	3.56	0.32	266	+0.32, −0.27	1.1
10,928	(c)	(c)	1.12	219	(d)	(d)

(a) Positive voltage refers to voltage spike produced as shock exits from specimen. Negative voltage refers to signal after shock exit from specimen (see Figure 13a).

(b) Guard ring shot; see Figure 13a.

(c) Transverse shot; electrodes are aluminum strips 6.35 mm wide and 6.35 mm apart; sample and electrodes are 4 mm high.

(d) Positive spike produced upon shock entrance into sample. Spike is followed by a gradual rise in voltage to a maximum of +0.17 volt 2μsec later. Shock transit time through specimen is 1.1 μsec.

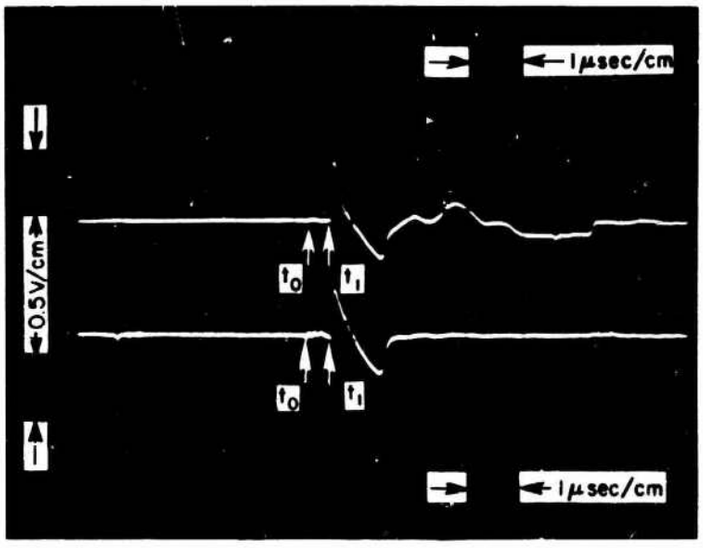

(a) RECORD FOR SHOT NO. 10,935
PASSIVE SHOT - NO APPLIED FIELD CsI AT 266 kbar
UPPER BEAM: CENTER ELECTRODE, Rs=3.5Ω
LOWER BEAM: GUARD RING ELECTRODE, Rs = 0.32Ω

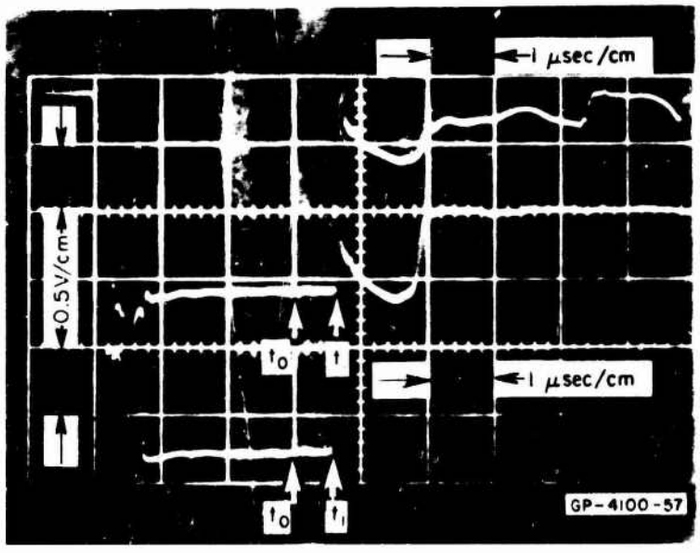

(b) RECORD FOR SHOT NO. 10,309
CsI GUARD RING SHOT WITH APPLIED FIELD AT 277 kbar
UPPER BEAM: CENTER ELECTRODE, Rs=3.40Ω
LOWER BEAM: GUARD RING ELECTRODE, Rs = 0.302Ω

FIG. 13 COMPARISON OF PASSIVE AND ACTIVE SHOTS FOR THE GUARD RING GEOMETRY
($t_1 - t_o$ = shock transit time)

One passive shot was fired with the transverse geometry (Shot No. 10,938). A positive-voltage spike was produced upon shock entrance into the sample, followed by a gradual rise in voltage to a maximum of +0.17 volt occurring 2 microseconds later (shock transit time was 1.1 μsec).* The validity of the record is in doubt because it was noisy. The signal did not resemble the signals obtained with the longitudinal geometry.

F. HOT SHOTS

The data from four successful hot shots are listed in Table I.† The records from Shot No. 10,503 and Shot No. 10,504 are reproduced in Figures 14a and b.

The NaCl record (Figure 14a) has several strange features. In the first place, the characteristic polarization signal produced as the shock traverses the specimen is conspicuously absent. The noise in the record beginning 1.2 μsec prior to the sharp rise in the signal corresponds to the shock reaching the 9-mil air gap separating the two halves of the driver plate. The mechanism for producing this signal is unknown, but we have observed signals in similar situations before. If the shock enters the crystal at the instant of the polarization signal produced in the gauge (*i.e.*, no shock tilt), the rapid increase in conductivity occurs about 0.1 μsec after the shock enters the backing electrode. On other shots, the onset of conduction corresponds within a few shakes§ to the shock reaching the electrode. After the initial rapid rise, which corresponds to a resistivity of 750 Ω-cm, the signal continues to rise less rapidly toward the baseline. The temperature of the NaCl in this case should cross the melting line as the pressure is relieved to zero; therefore this rapid drop in effective specimen resistance may be due to melting at the unsupported periphery of the crystal. The low resistivity of molten NaCl, ~ 1 Ω-cm (see Appendix B), makes it possible for a very little zero pressure material to effectively short out the remainder.

The CsI record is perhaps deceptively good. There is a positive spike as the shock exits from the specimen. Following this spike, the voltage across the shunt resistor remains nearly constant for about 0.6 μsec. In fact, the voltage does not change radically in the 3.6 μsec shown on the record. The resistivity measured after the initial positive spike is 1.8 Ω-cm.

---

* The conduction signal is on the order of 1 volt.

† Several shots were lost because of electrical leakage from heater wires to electrodes.

§ 1 shake = 0.01 μsec.

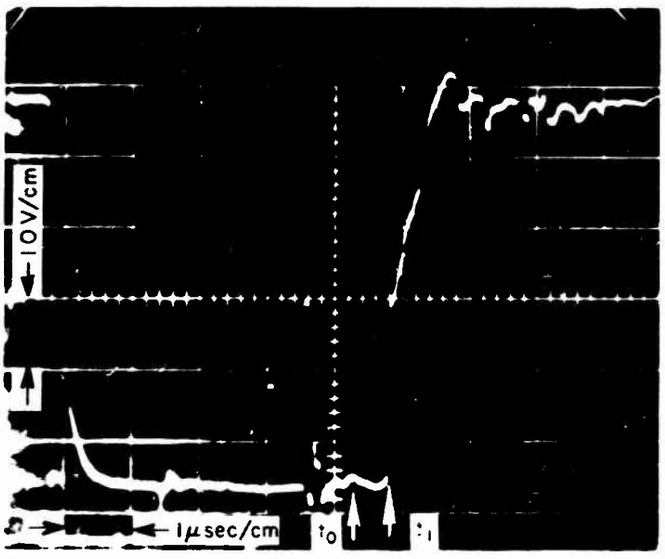

(a) SHOT NO. 10,504 — NaCl SPECIMEN PREHEATED TO 480°C

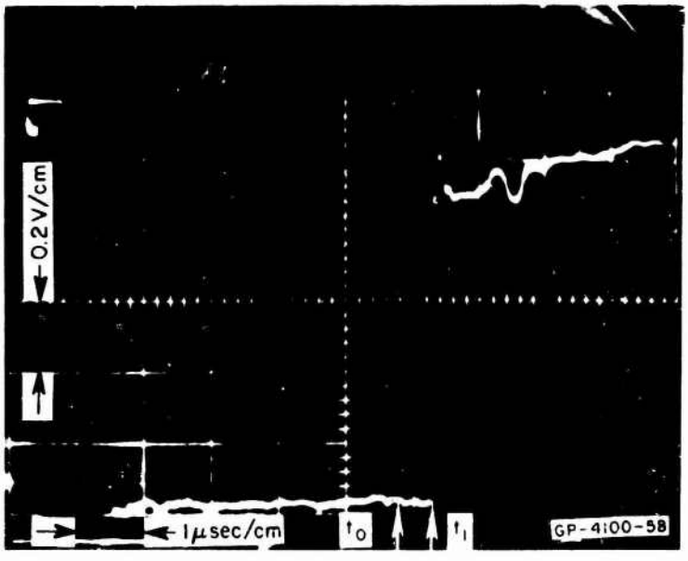

(b) SHOT NO. 10,503 — CsI SPECIMEN PREHEATED TO 420°C

FIG. 14 CONDUCTION SIGNALS IN PREHEATED SPECIMENS
($t_1 - t_0$ = shock transit time)

In Shot No. 10,931, CsI was preheated to 100°C and shocked to 230 kbar, and in Shot No. 10,932, CsI was preheated to 350°C and shocked to 232 kbar. In both cases, the records indicate negligible voltage across the shunt resistor after the shock exits from the sample, indicating resistivities of < 0.3 Ω-cm.

G. TRANSVERSE GEOMETRY

Four CsI shots were fired in the transverse geometry with the pressures ranging from 118 kbar to 255 kbar. The resistivities determined from these shots are at least an order of magnitude lower than the resistivity values from longitudinal geometry shots (see Section IV). The transverse-resistivity values range from 19 Ω-cm at 118 kbar (Shot No. 10,943) to 0.18 Ω-cm at 255 kbar (Shot No. 10,937). The value of 0.2 Ω-cm at 144 kbar in Shot No. 10,940 does not agree with the other three transverse shots. The shunt resistance used in this shot was too large so that the record indicates almost a short and is hence less reliable. The resistivities quoted here and in Table I are those determined just as the shock exits from the specimen.

The record from a typical shot (No. 10,937) is shown in Figure 15. The resistance increases as the shock traverses the specimen and then levels off as the shock exits and is nearly constant for 1 μsec, before relief waves reach the electrodes.

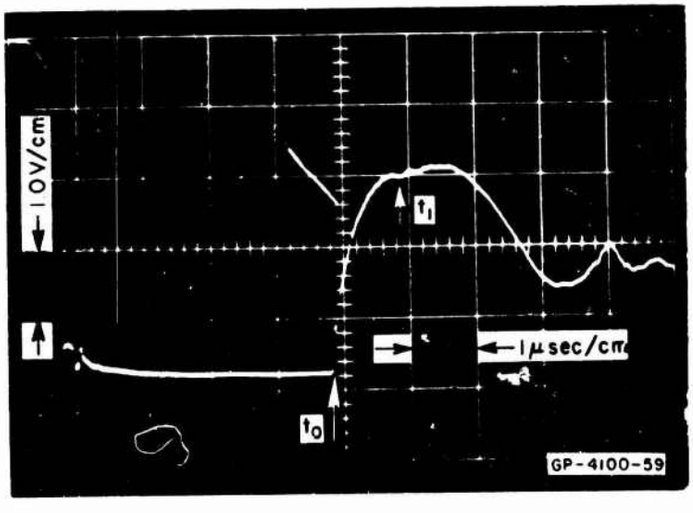

FIG. 15 SHOT NO. 10,937 CsI CONDUCTION SIGNAL IN TRANSVERSE GEOMETRY. Rs = 1.07 Ω
($t_1 - t_0$ = shock transit time)

For the constant-current measuring circuit, the sample resistance R_x was given by Eq. 1 as

$$R_x = R_s[(V/V) - 1]^{-1} \qquad (1)$$

The sample resistance can also be written in terms of the sample resistivity ρ, the cross-sectional area of the sample A, and the length of the current path L, as

$$R_x = \rho L/A \quad . \qquad (3)$$

If these two expressions are equated and ratio V/V is solved for, the result is

$$V/V_0 = (1 + R_s A/\rho L)^{-1} \quad . \qquad (4)$$

For the transverse geometry, the cross-sectional area of the conducting region varies with time as the shock wave traverses the specimen, and is given by

$$A = w(U - u)t \qquad (5)$$

where w is the width of the specimen, U is the shock velocity, u is the particle velocity behind the shock, and t is the time. In all the transverse-geometry shots, $w = L$. Substituting Eq. 5 into Eq. 4 yields

$$V/V_0 = [1 + R_s(U - u)t/\rho]^{-1} \quad . \qquad (6)$$

Figure 16 shows a plot of Eq. 6 for the parameters of Shot No. 10,937 compared with the observed value of V/V_0 taken from the record shown in Figure 15. The value of ρ used for Figure 16 is that determined from the record of Figure 15 at the time the shock leaves the crystal.

The two curves in Figure 16 do not have exactly the same shape. This result is possibly due to attenuation of the shock in the specimen. An alternative way of determining the resistivity would be to match the initial slopes of the two curves. If this is done, the resulting value of the resistivity is greater by a factor of two than the resistivity determined at the time of shock exit.

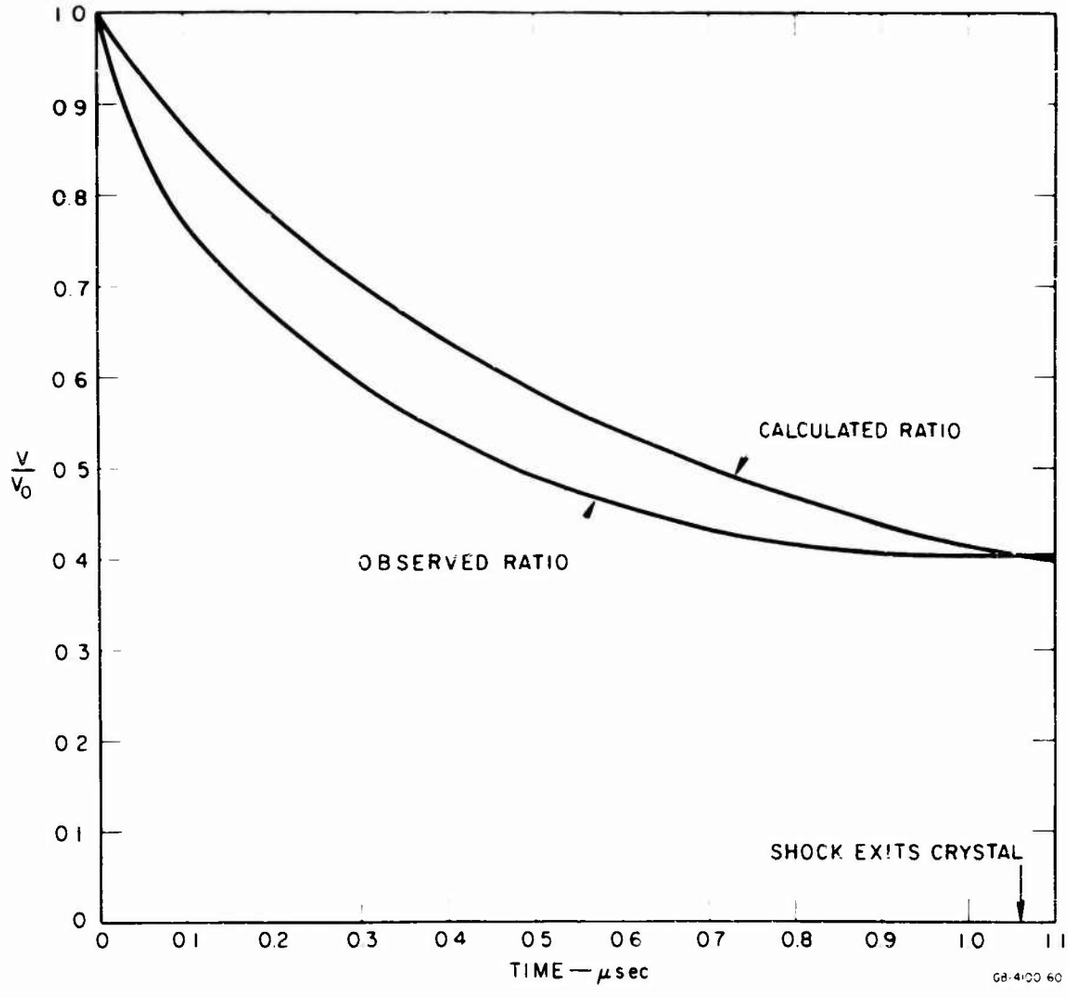

FIG. 16 PLOT OF CONDUCTION SIGNAL vs. TIME FOR THE CASE OF TRANSVERSE GEOMETRY. CALCULATED AND OBSERVED VALUES ARE SHOWN.

V DISCUSSION OF DATA

A. PRECISION

In Figure 17, oscilloscope records are shown for shots at high pressure with various values of shunt resistance. It seems clear that a large increase in electrical conductivity is indeed produced by a strong shock. The highest conductivity measured in the longitudinal configuration is near the upper limit of measurement. However, as discussed in Section IV, an order of magnitude higher conductivity should have been measurable using a high shunt resistance or a guard ring type backing electrode. The shape of the signals, however, is poorly understood, and therefore the interpretation of oscilloscope records is quite subjective. The signal amplitude may vary considerably during the first microsecond, particularly if the shunt resistance is small and approximately equal to the specimen resistance. Some light is shed on this by the passive shots discussed above, which indicate that at least part of the observed structure in the signal during the first μsec following shock transit is generated by the specimen.

The question naturally arises as to what influence this generated voltage has on the measurement of the specimen resistivity. In an attempt to answer this question, the results of active and passive shots (see Figure 13) for similar explosive systems and shunt resistors were superimposed on one another. This comparison suggests that the resistivity values which have been previously reported are not grossly in error.

There are several things which make this approach uncertain, however. The crystal thickness of the active shot was not identical to that of the passive shot used for comparison, nor were the shunt resistors of the compared shots identical. In a majority of the shots compared, the net voltage became positive* within 1 μsec after the shock exited from the specimen. Possibly more important is the fact that the conductivity

---

* A conduction signal is negative.

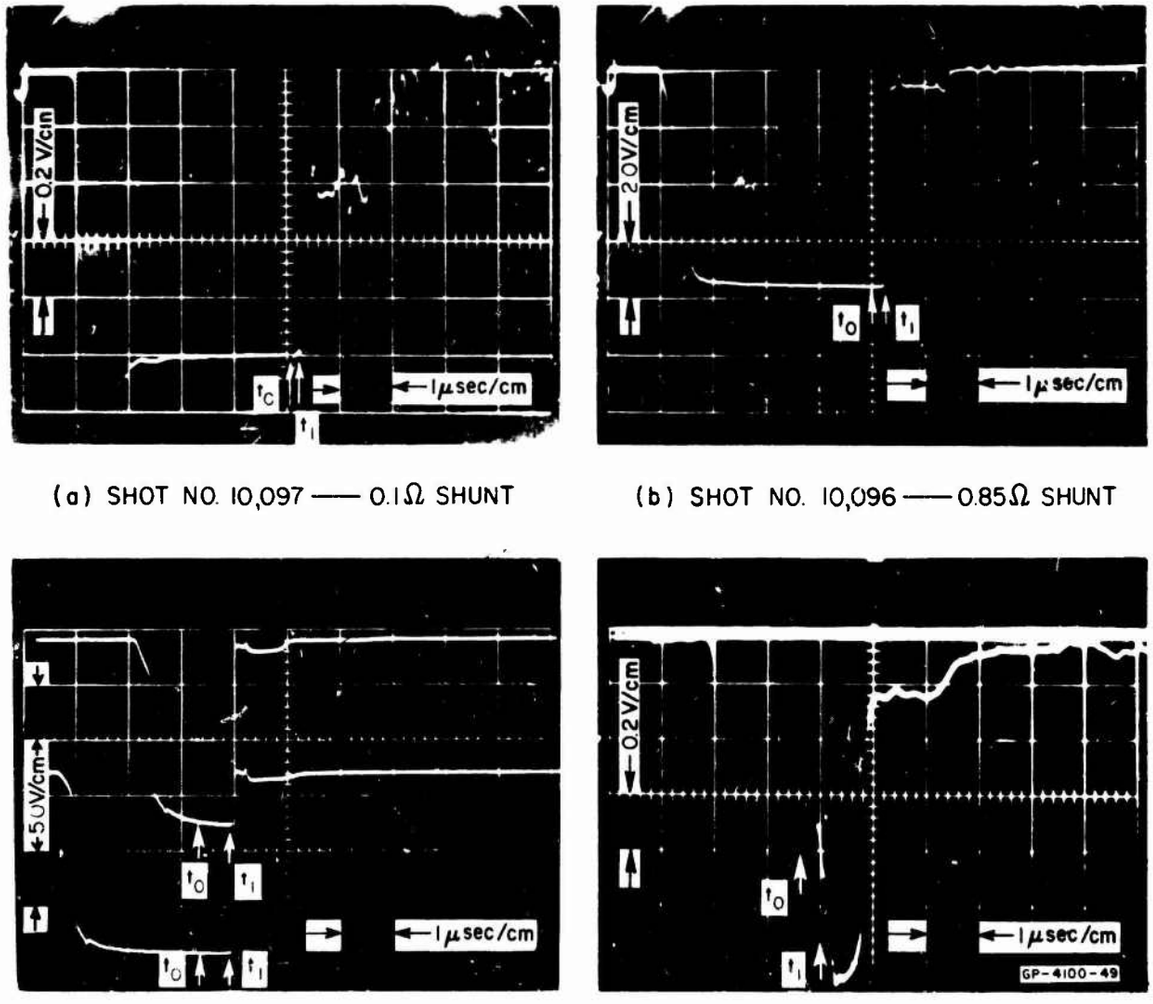

(a) SHOT NO. 10,097 —— 0.1Ω SHUNT

(b) SHOT NO. 10,096 —— 0.85Ω SHUNT

(c) SHOT NO. 10,314 —— 3.43Ω SHUNT

FIG. 17 COMPARISON OF RECORDS AT HIGH PRESSURE FOR DIFFERENT Rs
($t - t_c$ = shock transit time)

record is obtained with an electric field applied across the sample, whereas the record of the voltage generated by the specimen is obtained with no applied field. It is not known how the presence of an electric field will influence the voltage generated by the crystal.* It is particularly noteworthy in the passive records that a sharp positive spike is observed as the shock reaches the backing electrode. This justifies our neglect of this spike in interpreting earlier conductivity records.

The thermodynamic state of the specimen is also uncertain because of attenuation of the shock wave and the small impedance mismatch with the backing electrode. The temperature has a further uncertainty because it must be calculated using approximate thermodynamic parameters. At the beginning of this study, precise knowledge of the pressure was considered of secondary importance, and pressures reported in Report I were those measured with similar explosive assemblies on other projects. At the same time that the extreme pressure dependence of conductivity in CsI was being discovered, a resistance wire pressure gauge was being developed by another group in the Poulter Research Laboratories.[6] This gauge, used routinely on shots during the past year, not only indicates peak pressure but is believed to follow the subsequent pressure decay—how faithfully and for how long are subjects of current investigations. The duration of fidelity is primarily determined by gauge dimensions and the gauge used in this work should indicate shock decay at least semi-quantitatively during the first microsecond. We have used these data to correct indicated peak pressures to approximate average pressures in the specimen. This correction is indicated in Table III for the various explosive assemblies used. It should be noted that the data from Report I which are used in this report have also been corrected.

The pressure correction, although approximate, is obtained directly from gauge records. The corresponding corrections to the volume and temperature are not so straightforward. They have been estimated by assuming that the pressure behind the shock releases along the Hugoniot, *i.e.*, that the isentrope is approximated by the Hugoniot for the purpose of adjusting the volume and temperature. The result is that the volume and temperature corrections are underestimated, as shown by an example in Appendix C.

---

* In terms of the field required to produce a volume polarization equivalent to that produced by the shock, the field applied in these experiments should produce a negligible effect.

Table III

CORRECTIONS FOR SHOCK DECAY

EXPLOSIVE ASSEMBLY	PEAK STRESS IN DRIVER[a] (kbar)	SPECIMEN	PEAK STRESS IN SPECIMEN (kbar)	AVERAGE STRESS IN SPECIMEN[b] (kbar)
P-60 + 2" Baratol + 1/2" Al	150	CsI	127	125
P-60 + 1/2" Comp B-3 + 1" Baratol + 1/2" Al	183	KI	129	121
		CsI	161	154
P-60 + 2" TNT + 1" Al	221	CsI	198	187
P-60 + 2" TNT + 1/2" Al	223	KI	169	155
		CsI	214	205
P-60 + 2" Comp B-3 + 1" Al	267	KI	204	190
		CsI	244	230
P-60 + 2" Comp B-3 + 1/2" Al	305	NaCl	231	210
		KI	235	206
		CsI	283	250
P-60 + 2" 9404 + 1/2" Al	352	NaCl	261	226
		KI	275	238
		CsI	330	277
P-80 + 2" TNT + 1/2" Al	221	CsI(Hot)	189	181
P-80 + 4" 9404 + 1/2" Al	382	NaCl(Hot)	279	244
P-60 + 2" 9404 + 1/2" Al + 1/4" Hi-D	314(in Hi-D)	CsI	267	255
P-60 + 2" Comp B-3 + 1/2" Al + 1/4" Hi-D	257(in Hi-D)	CsI	214	203
P-60 + 2" TNT + 1/2" Al + 1/4" Hi-D	184(in Hi-D)	CsI	146	144
P-60 + 1/2" Comp B-3 + 1" Baratol + 1/2" Al + 1/4" Hi-D	156(in Hi-D)	CsI	121	118

[a] Except for hot shots, the peak stress in driver is the average of several shots.

[b] At time of measurement. This is taken to be 0.5 μsec after shock reaches backing electrode. The pressure decrease depends also on specimen thickness, the listed values being representative ones.

The Hugoniots for the specimen materials are from the work of Christian[8] and are shown in Figure 18, along with curves for aluminum and magnesium,[9] the electrode materials. The tabulated specimen pressures are for the *initial* transit of the shock through the specimen; no account is taken of the small mismatch at the specimen-backing electrode interface.

Calculated shock temperatures according to Christian[8] and Al'tshuler *et al.*[10] (NaCl only) are plotted in Figure 19. Christian used the simple technique given by Walsh and Christian[11] in which Grüneisen's parameter γ is assumed to be proportional to the volume V. The more elegant approach of Al'tshuler *et al.*[12] predicts γ decreasing less rapidly than V for CsI. Their calculated temperature data at low pressures look abnormally high, however, and the temperatures used in subsequent discussion will be those according to Christian.*

B. COMPARISON WITH OTHER WORKS

The work of Alder and Christian[1] which prompted this study was presented more quantitatively in a later paper by Alder.[13] These later data for NaCl, KI, and CsI are included in Figures 6-12; the agreement with our data is only fair.

In the case of CsI, Alder's 260-kbar point agrees with our transverse data, and his 190-kbar point agrees reasonably well with our longitudinal data. Alder and Christian reported that they observed no difference between longitudinal and transverse geometries, although the details of their experiments are sketchy. For KI, the agreement is fair; Alder's point falls within the scatter of our data.

The NaCl data disagree with both Alder and Al'tshuler *et al.*; our resistivities are at least an order of magnitude higher than theirs. Al'tshuler *et al.* indicate that the scatter in their data results from using crystals from different sources, and hence of presumably different purities.

* We have checked these temperatures and obtained reasonable agreement with Christian's.

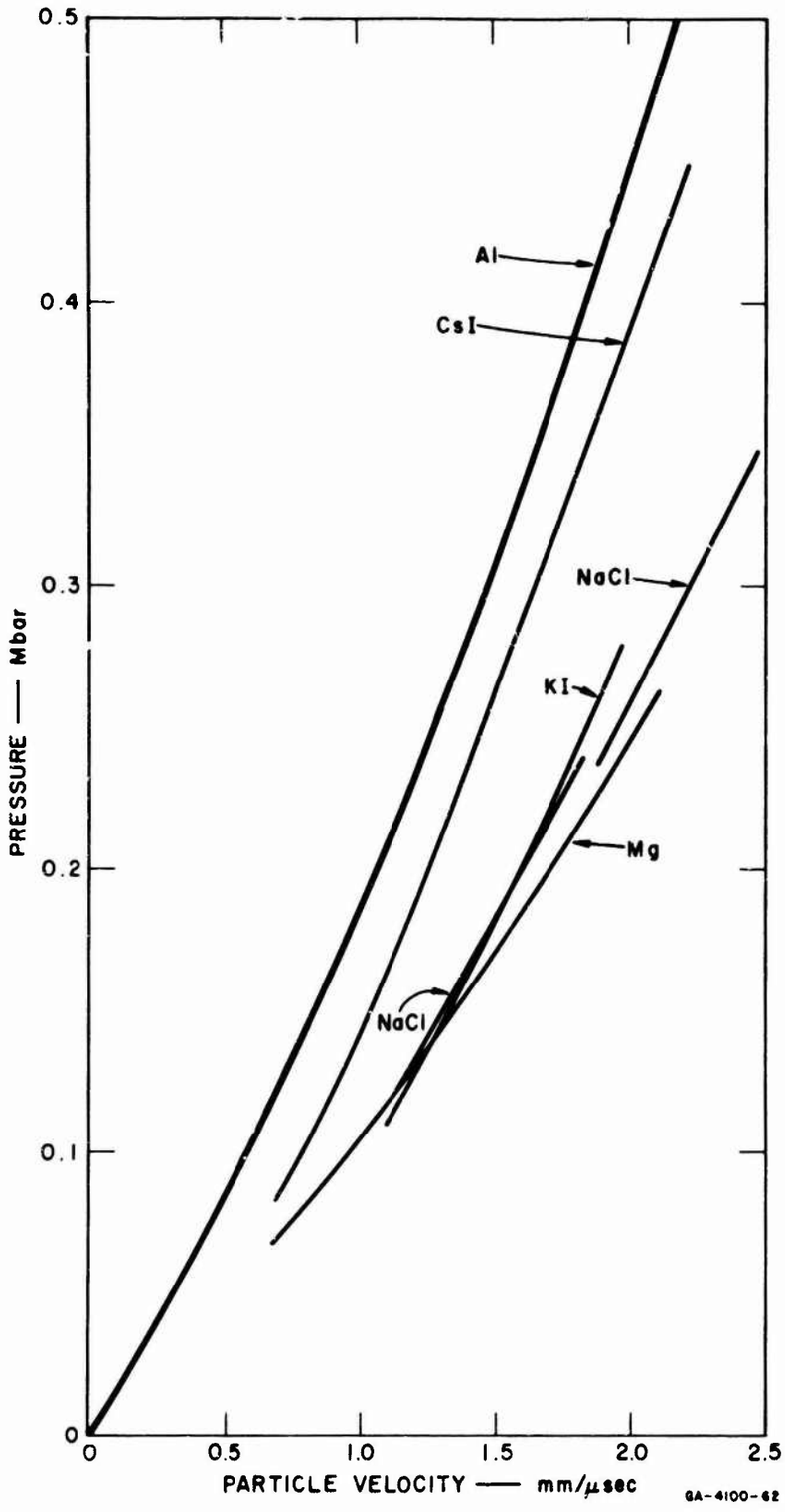

FIG. 18 PRESSURE vs. PARTICLE VELOCITY FOR NaCl, KI, CsI, Mg, AND Al

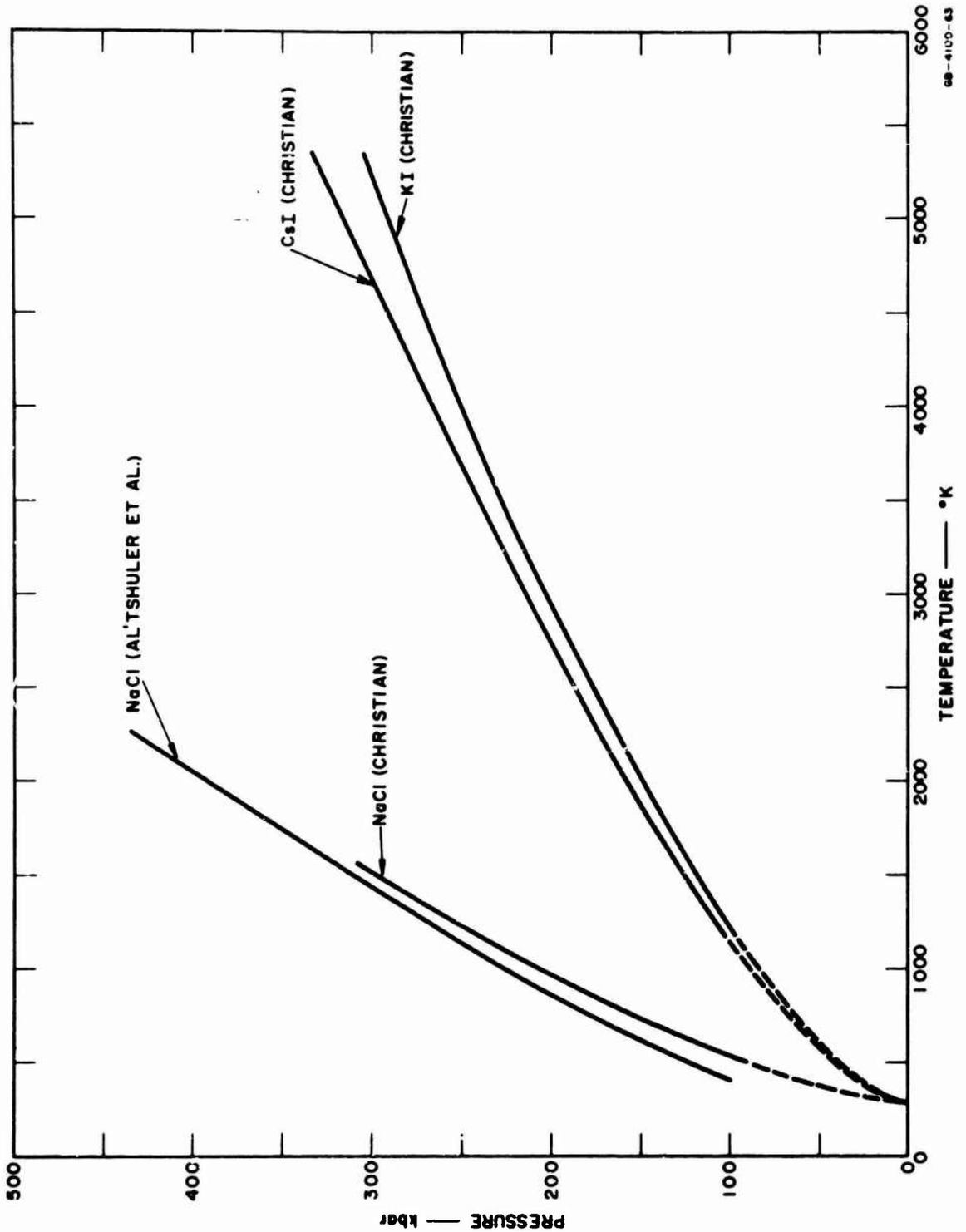

FIG. 19 PRESSURE vs. SHOCK TEMPERATURE FOR NaCl, KI, AND CsI

VI THEORETICAL CONSIDERATIONS

We have not yet determined what the conduction mechanism is; in the following discussion we consider the experimental results within the framework of two different hypotheses.

A. ELECTRONIC CONDUCTION

Alder[13] believes the current carriers are electrons and originally labeled the effect a "metallic transition." He suggested that the band gap is being decreased by pressure to such an extent that electrons are thermally excited into the conduction band. Considering the compressed specimen to be an intrinsic semiconductor and making assumptions about the mobility to arrive at a pre-exponential factor, he derived[13]

$$\rho(\Omega - \text{cm}) = (5.45/T)e^{Eg/2kT} \qquad (7)$$

where Eg is the band gap. The values of Eg given by Alder, corresponding to measured ρ and calculated T, are shown in Table IV with similar values calculated from our data. The values of Eg at 1 atmosphere (Eg°) are also given and, because they are determined optically, should be upper limits for the thermal band gaps.

The single point of Alder and Christian for NaCl agrees with our calculated band gaps. The data indicate that in the 200- to 244-kbar range the calculated thermal band gap is 3 to 5 ev compared to an optical band gap of 8.4 ev at atmospheric pressure and ambient temperature.

Alder and Christian's value of 4.1 ev at 160 kbar for KI agrees very well with our value of 4.4 ev at 155 kbar. KI undergoes a phase change at a pressure much less than 160 kbar and it is not known what band gap to associate with the high pressure phase. However, our data combined with Eq. 7 indicate an increase of about 2.2 ev in the band gap as KI is further compressed (and the temperature increased) to 242 kbar.

Table IV

BAND GAP CALCULATIONS

INVESTIGATORS[a]	SPECIMEN	σ (kbar)	V (cm^3/g)	T (°K)	ρ (Ω-cm)	SHOT GEOMETRY	BAND GAP - ev		
							Eq. 7	Eq. 9	$P = 0$
A & C	NaCl	220	0.3283	1000	1000 ± 200	Unknown	> 2.1	> 2.0	8.4 ± 0.7
D & M		199	0.330	1073	$> 5 \times 10^4$	Long.	> 3.0	> 2.8	
		225	0.323	1134	$> 0.9 \times 10^4$	Long.	> 2.8	> 2.6	
		244	0.326	2340[b]	186 - 753	Long.	4.6-5.1	3.6-4.1	
A & C	KI	160	0.2047	2250	50 - 150	Unknown	4.1	3.2	Unknown
D & M		155	0.2015	2325	131	Long.	4.4	3.4	
		190	0.1940	2971	116	Long.	5.7	4.1	
		214	0.1897	3640	10	Long.	5.5	3.4	
		242	0.1848	4500	6	Long.	6.6	3.7	
A & C	CsI	190	0.1436	2500	50 - 200	Unknown	4.7	4.2	6.3
		260	0.1349	3900	± 0.2	Unknown	≤ 3.4	≤ 1.0	
D & M		129	0.1515	1550	2.3×10^5	Long.	4.8	4.4	
		154	0.1484	2030	612	Long.	4.3	3.6	
		181	0.1482	3620[c]	1.8	Long.	4.4	2.3	
		187	0.1444	2665	30	Long.	4.4	3.2	
		230	0.1395	3460	12	Long.	5.3	3.4	
		262	0.1361	4375	5.1	Long.	6.3	3.5	
		298	0.1325	5600	6	Long.	8.4	4.3	
		118	0.1530	1390	19	Trans.	2.0	1.7	
		203	0.1425	2750	1.0	Trans.	3.0	1.6	
		255	0.1368	3965	0.2	Trans.	3.4	1.0	

[a] A & C = Alder and Christian; D & M = Doran and Murri.

[b] Specimen preheated to 480°C.

[c] Specimen preheated to 420°C.

For CsI, the band gaps calculated from the longitudinal shot data are consistently greater than those calculated from the transverse shot data. The 260-kbar point of Alder and Christian agrees with our transverse data, and their 190 kbar point agrees with our longitudinal data. As previously discussed, Alder and Christian report no difference in their data for longitudinal and transverse geometries.

Preheating the specimen was a first attempt to separate the volume and temperature dependence of the conductivity. The CsI shot with TNT was designed to reach approximately the same final temperature as a room temperature Comp B shot, but at a lower pressure (and larger volume). (The method of calculating the Hugoniot of the preheated material is the subject of Appendix A.) The calculated states and measured resistivities are shown in Table I. Assuming Eq. 7 to be valid, Eg is given in terms of the resistivities at two different temperatures but the same volume by

$$Eg = \frac{2k \ ln \ (\rho_1 T_1 / \rho_2 T_2)}{\frac{1}{T_1} - \frac{1}{T_2}} \qquad (8)$$

Using Eq. 8 and the values in Table I gives Eg = 4.2 ev for CsI. Using Eq. 7 separately for each point yields values of Eg of 4.3-4.4 ev, but the use of Eq. 8 seems most valid because the questionable magnitude of the pre-exponential term is not involved.

Following the initial apparent decrease in the band gap, the data from both geometries indicate, as for KI, an increase in band gap as the shock strength is increased. Three obvious causes of such a trend are: (1) the measured values of resistivity are too high at high pressures; (2) The calculated temperatures are too high; and (3) Eq. 7 is not of the proper form. We have convinced ourselves that our experimental technique is capable of measuring resistivities an order of magnitude lower than those observed. Although there is considerable uncertainty in the calculation of the shock temperature, there is no reason to believe that the calculated values used here are excessive; indeed, the temperatures published by Al'tshuler *et al.* are considerably higher. Equation 7 certainly is vulnerable to criticism. The principal assumptions involved in its derivation are that the specimen behaves as an intrinsic semiconductor, and that the mobility varies as $T^{-1/2}$. In Appendix D an alternative expression is derived, which retains the former assumption but replaces

the latter by a $T^{-2.5}$ dependence. This more closely approximates the experimental data for polar semiconductors, such data being used also to determine a pre-exponential constant (see Appendix D). The result is

$$\rho = (1.2 \times 10^{-5}) T e^{E_g/2kT} . \qquad (9)$$

Band gaps calculated from Eq. 9 are also included in Table IV. The band gaps are lower than those calculated from Eq. 7, and the change with increasing pressure is not as great.

Of course no possible effects of shock compression on the crystal lattice—*e.g.*, the influence on the mobility of shock-produced point defects, dislocations, perturbed phonon spectrum—are included in Eqs. 7 and 9. Again, if impurity conduction is important, Eqs. 7 and 9 are not applicable.

The data from the longitudinal and transverse geometries lie on separate curves, the transverse geometry indicating the lower resistivities. Two possible mechanisms are suggested for a directional dependence. To the extent of its ability to support a shear stress, the cubic symmetry of the crystal is perturbed under compression by a plane shock wave; hence the conductivity need not remain a scalar quantity. Also, the mobility is influenced by lattice imperfections; the distribution of dislocations, for example, is not expected to be isotropic.

This interpretation in terms of decrease in band gap with lattice compression is in conflict with the theoretical work of Flower and March.[5] They calculated the band gap of CsI as a function of isotropic compression of the lattice to 250 kbar and concluded that any change was negligible.

B. IONIC CONDUCTION

Al'tshuler *et al.*[10] suggested that the conductivity they observed in NaCl at very high pressures was ionic in nature. This conclusion was based on a linear $ln\rho$ *vs.* $1/T$ plot giving an activation energy of 1.2 ev, a magnitude similar to that observed for ionic conductivity at 1 atmosphere.[14] They gave no discussion in terms of a pressure or volume dependence.

Our data for NaCl are too few and at too low a pressure to confirm Al'tshuler's suggestion. Figure 10 shows a plot of Al'tshuler's data (the dashed lines are his). The resistivity determined for our hot shot

is an order of magnitude greater than his at the same temperature. It is tempting to conclude that this fact indicates a volume dependence of the resistivity—the volume for our hot shot being greater than the volume for Al'tshuler's room temperature shot. This is unwarranted, however, because our lower pressure room temperature shots also exhibit higher resistivities than those of the Russians.

For both KI and CsI, our data on a log ρ *vs.* $1/T$ plot can be roughly fitted, at the higher temperatures (and higher pressures), by a straight line (see Figures 11 and 12). The activation energy determined from the slope is 1.6 ev for KI and 1.1 for CsI. The data for CsI are compared with zero pressure data in Figure 20.

At 1 atmosphere, the conductivity of the alkali halides is by diffusion of ions (usually positive at lower temperatures, with the contribution of negative ions increasing with temperature) via a vacancy mechanism. The magnitude of conductivity is determined by the concentration of vacancies and by their mobility. If the crystal is maintained in the thermodynamic equilibrium, the conductivity will be intrinsic at high temperature, *i.e.*, independent of the impurity content. Below some fairly well defined temperature (which increases with impurity content), the concentration of vacancies is determined primarily by the presence of divalent impurities; this region is called extrinsic.

Although the equilibrium temperature dependence of conductivity for the materials used in this study are relatively well known (see Figure 20), the pressure dependence is not. The only measurements on ionic solids above 1 kbar are those of Pierce[16] to 9 kbar on the chlorides of Na, K, and Rb. These measurements are in the extrinsic range; furthermore, the pressure dependence is characterized by an activation volume (see Appendix B for discussion of ionic conductivity) which shows no systematic pressure dependence in the low-pressure range available to Pierce, but which must certainly be pressure-dependent. Hence Pierce's data merely provide a starting point for estimating the pressure dependence at the pressures of interest. Such an estimate is discussed in Appendix B. The result is that one cannot say much more than that for weak shocks (low temperatures), the pressure dependence overshadows the temperature dependence, and that the opposite is true for strong shocks (high temperatures). Thus the conductivity should first decrease and then increase as the shock strength is increased. One might expect, then, that the usual

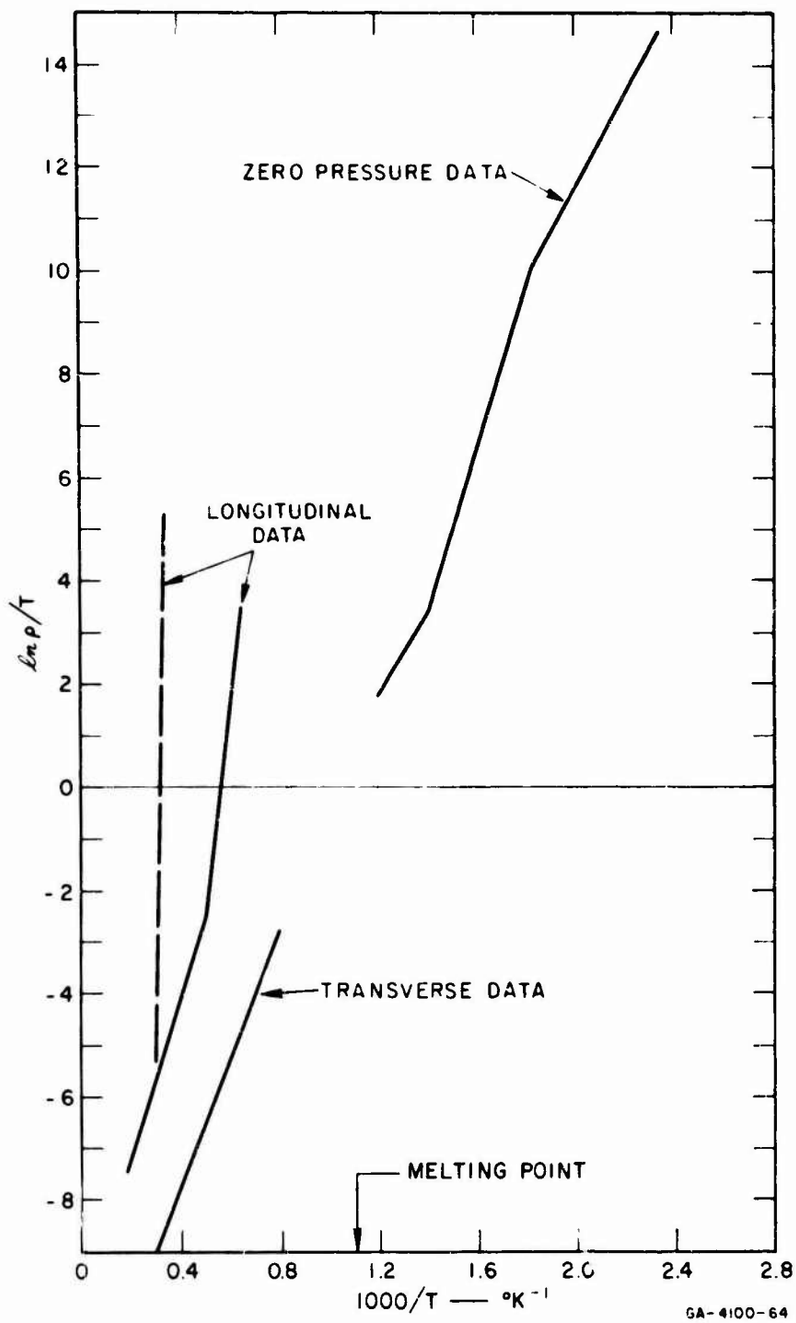

FIG. 20 PLOT OF $\ln\rho/T$ vs. $1/T$ FOR CsI SHOWING HIGH PRESSURE DATA IN RELATION TO ZERO PRESSURE DATA.[15]

$\ln \sigma T$ vs. $1/T$ plot (σ = conductivity) for shock experiments would have a larger slope at high temperatures (corresponding to strong shocks) than a similar plot at $P = 0$, and hence would have an abnormally high apparent value of activation energy.

Another approach to the problem of pressure dependence is to assume that, at equilibrium, the conductivity is determined by T/T_m, where T_m is the melting point—*i.e.*, a corresponding states approach. Again, because the ratio of Hugoniot temperature to melting temperature first decreases and then increases as shock strength is increased, the conductivity would do likewise.

There is still another argument. The pressure dependence of the conductivity of molten salts is probably small (see Appendix B). It seems reasonable that the conductivity change on melting (increases by $\sim 10^3$ at $P = 0$)[17] should be relatively insensitive to pressure. Hence the pressure dependence of conductivity in the solid, near the melting point, should be small.

The reason for this emphasis on the region near the melting curve is that the temperatures behind the strong shock waves producing high conductivity in KI and CsI are probably near the melting point.

The only pertinent data on melting curves of alkali halides are those of Clark, who made measurements to 25 kbar on the sodium halides and the alkali chlorides.[18] There is little choice but to use the two-parameter Simon equation, with Clark's values of the constants,* to extrapolate an order of magnitude in the pressure. The results of such extrapolations are shown in Figure 21 along with the calculated shock temperatures. The uncertainties in the melting curve for CsCl-II are those indicated by Clark; the uncertainty is similar for NaCl and NaI and larger for KCl-II (one parameter was assumed because phase II was present only over a 5-kbar region). It must be concluded that, if there is time for melting to occur, there is a good chance that our specimens are in the molten state for the strongest shocks. Available evidence indicates that melting can occur, at least during pressure release, in the brief duration of a shock experiment. This evidence—admittedly indirect—is the failure of measured

* Recorrecting Clark's thermocouple measurements of temperature for the effect of pressure, using the recent work of Bundy and Strong,[19] has negligible effect on the melting curves in comparison with the uncertainties in determining the parameters in the Simon equation.

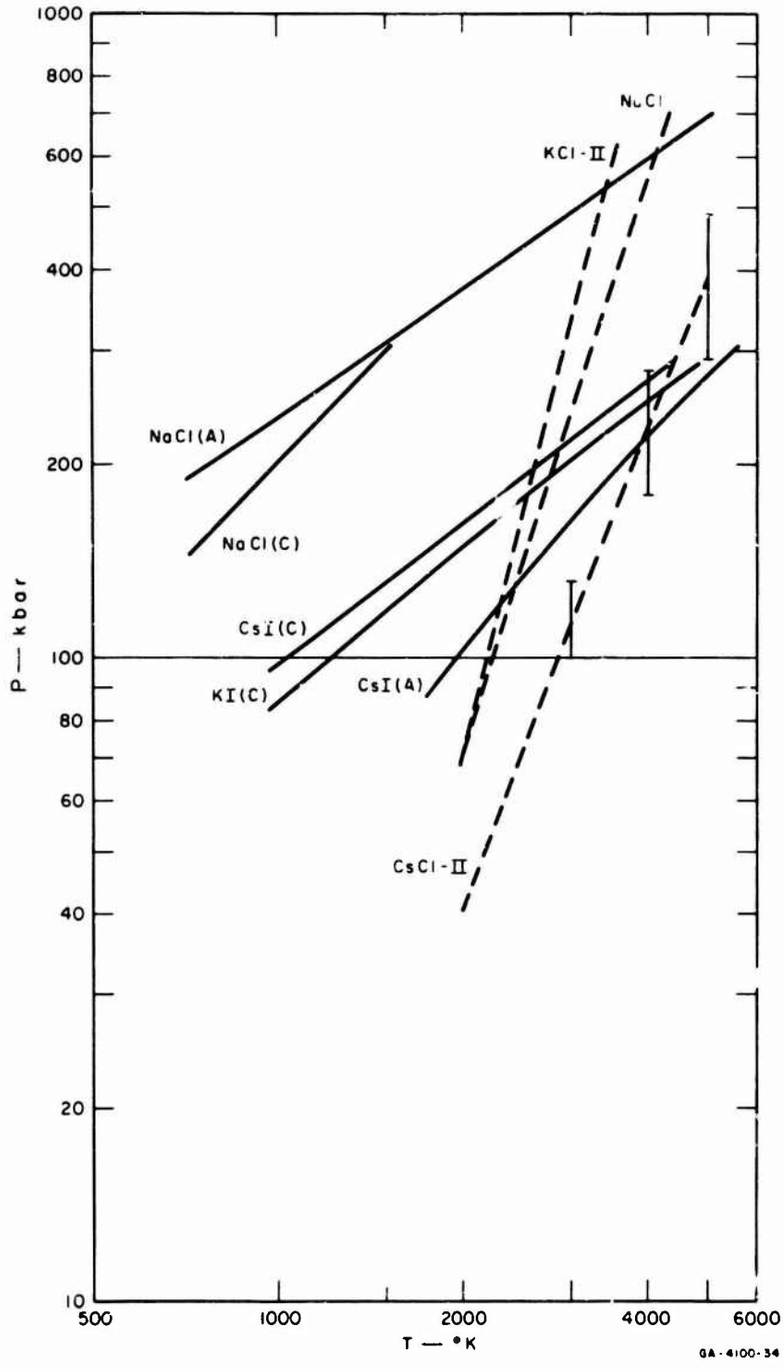

FIG. 21 HUGONIOT TEMPERATURES (solid lines) ACCORDING TO CHRISTIAN[8] (C) AND AL'TSHULER et al,[10,12] (A). Melting curves (dashed lines) extrapolated from 25 kbar data of Clark.[18] The suffix II refers to the polymorph having the CsCl structure. Presumably the iodides and chlorides have nearly identical melting curves (true for Na).

free-surface velocity to equal twice the particle velocity (as determined by the impedance mismatch technique) for low melting-point metals[9] and for the alkali halides[8] themselves.

Yaffe and Van Artsdalen[20] have measured the conductivities of several molten salts at 1 atmosphere. They found values of the order of 1 $(\Omega\text{-cm})^{-1}$ with a very small temperature dependence, which would result in activation energies of 0.1-0.2 ev for NaCl, CsI, and KI, one order of magnitude lower than for the solid state.*

In summary, we might expect the following behavior of ionic conductivity assuming thermodynamic equilibrium. The temperature increases slowly for weak shocks; we expect the pressure effect to be dominant and the conductivity to decrease with increasing shock strength. At higher shock strengths the temperature begins to increase so rapidly that the pressure effect becomes minor and the downward trend of conductivity is reversed. In particular, near the melting line we expect conductivities of the order of 10^{-3} to 10^{-4} $(\Omega\text{-cm})^{-1}$, as at 1 atmosphere; likewise, if melting occurs we expect ~ 1 $(\Omega\text{-cm})^{-1}$ and increasing the shock strength should have little effect.

The heated CsI shot is consistent with the melting hypothesis. It may be that a specimen initially at room temperature melts when shocked to 270 kbar. If this is so, it will certainly melt when shocked to approximately the same temperature at a lower pressure ($\sim$180 kbar). The corresponding resistivities are 5 and 1.8Ω-cm, respectively. The data can also be used to compare resistivities at different temperatures but the same volume. Using Eq. B-3, the activation energy is given by

$$\Delta G = \frac{k \ ln \ (\rho_1 T_2 / \rho_2 T_1)}{\left(\frac{1}{T_1} - \frac{1}{T_2}\right)} \qquad (10)$$

the ionic analog of Eq. 8. From the data of Table I and Eq. 10, ΔG = 2.5 ev (at a volume corresponding to 154 kbar on the room temperature Hugoniot) which is double the value of 1.25 ev found for CsI in the intrinsic region at zero pressure. However, if melting is occurring,

* It has recently been observed that the conductivity of molten salts may *decrease* with increasing temperature well above the melting point.[2]

most of the drop in resistivity can be ascribed to it. Add to this a possible pressure-produced increase in resistivity contributing to the low temperature point, and one can easily rationalize the larger value of ΔG. What is not so easy to rationalize, if melting is occurring, is the discrepancy between the longitudinal and transverse experiments and the discrepancy between experiments on different specimens, which we have tried to ascribe to variations in impurity content or a dependence on crystallographic orientation.

Implied in this discussion is the assumption that the pressure is hydrostatic and the process of compression is quasi-static. Let us consider the consequences of admitting that we have shocked the crystal. In the first place, dislocations are presumably being produced and driven at high velocity and they may be leaving vacancies and interstitials behind. Both the dislocations and the point imperfections can contribute to the conductivity. In the second place, our measurements are made during the first μsec behind the shock front, which seems a rather short time in which to consider a process quasi-static. However, the jump frequencies become very high at high temperatures, and the dislocations provide a large concentration of sources and sinks for point imperfections, so that thermodynamic equilibrium may be possible in the shocked solid near the melting line. This will further enhance the increase of conductivity to be expected as the shock strength (and hence temperature and, specifically, T/T_m) is increased.

C. OTHER POSSIBLE MECHANISMS

Other conduction mechanisms include the following possibilities:

1. Both electrons and ions may be contributing to the current, perhaps in different temperature ranges.
2. Conduction by electrons contributed by impurities. It would then be coincidental that CsI from Harshaw and Isotopes, Inc. give similar results.
3. Conduction by electrons produced at the electrodes by photo- or thermal-emission due to the hot specimen. This is not a possible conduction mechanism because the electrons are not free to move through the crystal; it might however, play a role in the polarization phenomenon.

VII CONCLUSIONS

The alkali halides, CsI and KI, experience rapid increases in electrical conductivity when subjected to shock waves of amplitude greater than 165 kbar and 185 kbar respectively. The corresponding shock temperatures are estimated to be 2470°K and 2600°K. The results of transverse geometry shots with CsI (and KI—see Report I) suggest that the conductivity is dependent on the current direction relative to the direction of shock propagation (see Section IV). The discrepancy between the CsI data from Report I and the present data suggest also a dependence on crystal orientation and/or crystal purity.

NaCl shocked to comparable pressures has a much lower temperature (due primarily to its large specific heat), and its resistivity is $\geq 10^4$ Ω-cm at 225 kbar. If the specimen is preheated to 480°C and shocked to 244 kbar, the resistivity is ~ 470 Ω-cm. This is the only shot for which we were able to observe appreciable conductivity in NaCl.

We have not yet determined the conductivity mechanism. The data are not consistent with either of the two models considered—an intrinsic semiconductor with band gap narrowed by compression of the lattice, or a simple ionic solid which is melting at the high temperatures produced behind the shock front.

VIII SUGGESTIONS FOR FURTHER WORK

1. Extend the measurements to specimens compressed along crystallographic directions other than those presently employed.

2. Make additional conductivity measurements in a transverse geometry, *i.e.*, in a direction parallel to the shock front. Preliminary results indicate a directional dependence of the conductivity.

3. Extend conductivity measurements on material in different P-V-T states, using specimen preheating and shock reflection techniques.

4. Study crystals in which the character and concentration of defects have been altered by irradiation, plastic deformation, or doping.

5. Extend work on NaCl to higher temperatures and compressions.

6. Study the polarization signal to determine its origin and to reduce the uncertainty in interpreting the conductivity records.

APPENDIX A

ESTIMATION OF SHOCKED STATES IN PREHEATED SPECIMENS

APPENDIX A

ESTIMATION OF SHOCKED STATES IN PREHEATED SPECIMENS

Starting from the Hugoniot with initial state (V_0, T_0), we will estimate the Hugoniot for initial state (V_0', T_0'), where the primed initial state is obtained from the unprimed initial state by heating at $P = 0$ (Figure A-1).

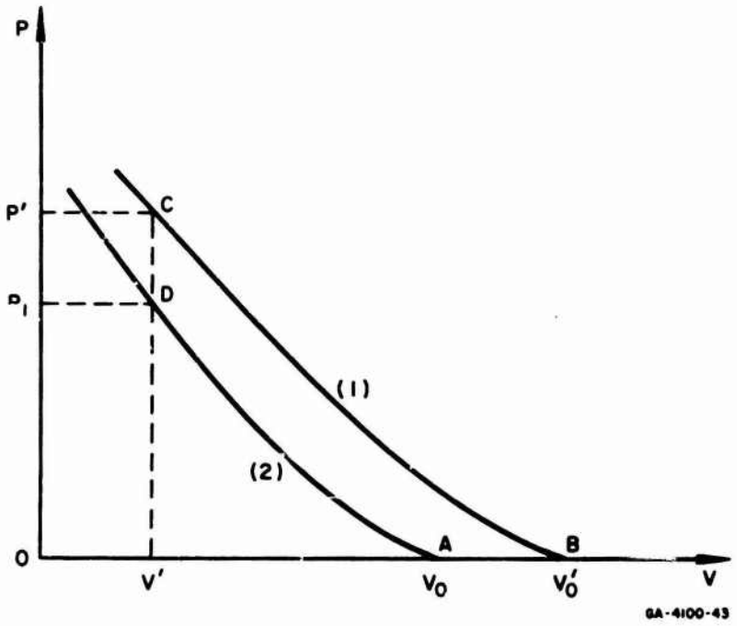

FIG. A-1 ILLUSTRATING CALCULATION OF HUGONIOT OF PREHEATED MATERIAL (1) FROM HUGONIOT OF ROOM TEMPERATURE MATERIAL (2)

If β = thermal expansion coefficient,

$$V_0' = V_0 + \int_{T_0}^{T_0'} V\beta dT = V_0[1 + \bar{\beta}(T_0' - T_0)] \qquad \text{(A-1)}$$

We will assume that $(\partial P/\partial E)_V$ = constant. That is, in the Mie-Grüneisen form of equation of state

$$P_2 - P_1 = \frac{\Gamma}{V}(E_2 - E_1) \quad , \qquad \text{(A-2)}$$

we will assume $\Gamma/V = (\Gamma_0/V_0)$ = constant. This is a drastic assumption, but seems to be about as valid a volume dependence for Γ as that determined by other means.

At any (P,V) point on a Hugoniot with initial state $(P_0, /V_0)$ the internal energy E is given in terms of the initial internal energy E_0 by

$$E - E_0 = \frac{1}{2}(P + P_0)(V_0 - V) \quad . \tag{A-3}$$

Letting $P_0 = 0$, we now apply Eqs. A-3 and A-2 to determine the energy at point C by two different paths:

$$\text{Path ADC:} \quad E' = E_0 + \frac{1}{2} P_1(V_0 - V') + \frac{V_0}{\Gamma_0}(P' - P_1) \quad . \tag{A-4}$$

$$\text{Path ABC:} \quad E' = E_0' + \frac{1}{2} P'(V_0' - V') = E_0 + \int_{T_0}^{T_0'} C_p\, dT + \frac{1}{2} P'(V_0' - V')$$

Using Eq. A-1,

$$E' = E_0 + \bar{C}_p(T_0' - T_0) + \frac{1}{2} P'[(V_0 - V') + V_0\bar{\beta}(T_0' - T_0)] \quad . \tag{A-5}$$

Equating (A-4) and (A-5) and solving for P' yields

$$P' = \frac{P_1\left[\frac{1}{2} V_0(1 - V'/V_0) - V_0/\Gamma_0\right] - \bar{C}_p(T_0' - T_0)}{\left[\frac{1}{2} V_0(1 - V'/V_0) - V_0/\Gamma_0\right] + \frac{1}{2} V_0\bar{\beta}(T_0' - T_0)} \tag{A-6}$$

and $$T' = T_1 + (E' - E_1)/C_V = T_1 + V_0(P' - P_1)/\Gamma_0 C_V \quad . \tag{A-7}$$

Then, given the material constants Γ_0, $\bar{C}_p$, $\bar{\beta}$, and the Hugoniot through $(P_0 = 0,\ V_0)$, we can calculate the pressure P' and temperature T' along a Hugoniot through $(P_0 = 0,\ V_0')$. The procedure is to assume a V', calculate P' from Eq. (A-6), and then T' from Eq. (A-7).

To determine the shocked states actually reached in a given system, it is necessary to map the new P, V Hugoniot into the P-u plane. The particle velocity u' corresponding to $(P',\ V')$ is given by

$$u' = [P'(V_0' - V')]^{1/2} \tag{A-8}$$

APPENDIX B

PRESSURE DEPENDENCE OF IONIC CONDUCTIVITY

APPENDIX B

PRESSURE DEPENDENCE OF IONIC CONDUCTIVITY

At $P = 0$, conduction in the alkali halides is completely ionic; the mechanism for this is the diffusion of vacancies.[17] The conductivity depends on the density n of carriers and on the mobility μ (the drift velocity per unit electric field). We will identify n with the concentration of vacancies of one sign, because generally the mobility of one ion is significantly greater than that of the other.

For a pure crystal, there is an equilibrium value of n (nonzero for $T > 0$) determined by the free energy of formation ΔG_f of a vacancy pair:

$$n \propto e^{-\Delta G_f / 2kT} \tag{B-1}$$

The factor of two arises because charge neutralization requires that vacancies be formed in pairs, and the total number of ways to choose a pair of vacancies is the square of the number of ways to produce a single vacancy. Even for the highest purity crystals available, n is governed by Eq. B-1 only for temperatures above perhaps 300°C, called the intrinsic region. Below this temperature is the extrinsic region where n is determined by certain impurities. The most important of these impurities are those with a valence of +2 (*e.g.*, $CaCl_2$ in a NaCl lattice) because, for each divalent ion which takes a regular lattice position, there must be a positive ion vacancy to maintain charge neutrality.

The mobility is determined by the jump frequency Γ, which depends on the difference in free energies ΔG_m of the activated state (ion midway between two lattice sites) and the ground state (ion at a normal lattice site). The relation is of the form

$$\mu \propto \frac{\Gamma}{T} \propto \frac{1}{T} e^{-\Delta G_m / kT} \tag{B-2}$$

The exact form of the pre-exponential factor depends on the model used in the calculation. The conductivity is then

$$\sigma = \frac{\sigma'_\infty}{T} e^{-\Delta G/kT} , \tag{B-3}$$

where $\Delta G = 1/2\ \Delta G_f + \Delta G_m$. For comparison with experiment, the temperature dependence of the coefficient is often neglected and the expression

$$\sigma = \sigma_\infty e^{-\Delta G/kT} \tag{B-3a}$$

is written.

The pressure dependence of σ can be expressed[22] by an activation volume ΔV defined by $\Delta V = (\partial \Delta G/\partial P)_T$. Differentiating Eq. B-3a:

$$\left(\frac{\partial\ ln\ \sigma}{\partial P}\right)_T = \left(\frac{\partial\ ln\ \sigma_\infty}{\partial P}\right)_T - \frac{\Delta V}{kT} \tag{B-4}$$

Now $\sigma_\infty \propto Na^2\nu$, where N = number ions of given sign/cm^3 $\propto V^{-3}$, a = lattice constant $\propto V^{1/3}$, and ν = vibration frequency. Let $\nu \propto \theta$, the Debye temperature, so that $\nu \propto V^{-\gamma}$ where γ is the Grüneisen parameter defined by $\gamma = -(d\ ln\ \theta)/(d\ ln\ V)$. Therefore

$$\sigma_\infty \propto Na^2\nu \propto V^{-3+2/3-\gamma} \tag{B-5}$$

and

$$\left(\frac{\partial\ ln\ \sigma_\infty}{\partial P}\right)_T = -\left(\gamma + \frac{7}{3}\right)\left(\frac{\partial\ ln\ V}{\partial P}\right)_T = \left(\gamma + \frac{7}{3}\right)/B_T \tag{B-6}$$

where B_T is the isothermal bulk modulus.

The ratio of the magnitudes of the two terms on the right side of Eq. B-4 is then

$$\frac{\left(\gamma + \frac{7}{3}\right)kT}{B_T \Delta V} \equiv r \tag{B-7}$$

At $P = 0$ and room temperature, $\gamma \cong 2$, $B_T \cong 7 \times 10^{11}$ dyne/cm^2, $\Delta V = (\Delta V)_0 \cong$ volume/ion $\cong 1 \times 10^{-23}$ cm^3. Then at $P = 0$, $T = 300°$K, $r = r_0 \cong 0.03$.

From the work of Keyes[23] we deduce that r should never get much larger. Keyes concludes that (approximately)

$$B_T \Delta V = s \Delta G \tag{B-8}$$

Since s = constant and γ changes little, $r \propto T/\Delta G$. In integrated form, Eq. B-8 becomes

$$\Delta G = (\Delta G)_0 \left(\frac{V_0}{V}\right)^s \tag{B-9}$$

which is strictly true only at constant T. However, it is consistent with Eq. B-8 to assume that ΔG is a function only of volume. Thus

$$r \propto TV^s \tag{B-10}$$

T cannot increase by more than a factor of ~3 at $P = 0$ without melting occurring. Increasing P enables T to be increased but V decreases and, since s is in the range of 2 to 4, r should increase little, if any.

This argument is presented to justify dropping the first term on the right side of Eq. B-4. Doing so and integrating gives

$$\sigma = \sigma_T e^{-P\overline{\Delta V}/kT} = \sigma_\infty e^{\left[-(\Delta G)_0 - P\overline{\Delta V}\right]/kT} \tag{B-11}$$

where $\overline{\Delta V} \equiv \frac{1}{P}\int_0^P \Delta V dP$ and subscript 0 indicates $P = 0$.

Equation B-11 provides an atomistic approach to the consideration of the pressure dependence of σ, because the activation volume can be interpreted in terms of atomic volumes with fair success.[22]

Our problem is to make a reasonable estimate of an upper limit for ionic conductivity at pressures and temperatures far exceeding the range of available measurements. Since σ increases with T, we will confine our analysis to the region of the melting curve.

Our first approach was to use Eq. B-11, making the arbitrary assumption that

$$\Delta V = \frac{V}{V_0} (\Delta V)_0 \tag{B-12}$$

Equation B-11 can be expressed in terms of the volume along the melting curve by using the Simon expression[24] to relate P and T,

$$P = A \left[\left(\frac{T_m}{T_{m0}} \right)^a - 1 \right] \tag{B-13}$$

and the Murnaghan expression[25] to relate P and V

$$P = B \left[\left(\frac{V_0}{V} \right)^b - 1 \right] , \quad B = B_T / b \tag{B-14}$$

Both Eqs. B-13 and B-14 are here treated as empirical relations. Combining Eqs. B-11 and B-14 gives

$$\ln \frac{\sigma_\infty}{\sigma} = \frac{(\Delta G)_0}{kT_{m0}} \left\{ 1 + \frac{B(\Delta V)_0}{C_1 (\Delta H)_0} \left(\frac{V}{V_0} \right) \left[\left(\frac{V_0}{V} \right)^b - 1 \right] \left[\left(\frac{V_0}{V} \right)^b + C_2 \right]^{-1/a} \right\} \tag{B-15}$$

where $C_1 \equiv (B/A)^{1/a}$, $C_2 \equiv (A/B) - 1$.

In searching for an improvement over the assumption of Eq. B-12, the relation (Eq. B-9) of Keyes was discovered. Combining Eqs. B-9, B-11, B-13, and B-14 gives

$$\ln \frac{\sigma_\infty}{\sigma} = \frac{(\Delta G)_0}{kT_{m0}} \frac{1}{C_1} \left(\frac{V_0}{V} \right)^s \left[\left(\frac{V_0}{V} \right)^b + C_2 \right]^{-1/a} \tag{B-16}$$

Equations B-15 and B-16 have been evaluated for sodium.[26] The constants B and b are from fits to Bridgman's isothermal data,[27] but the variation from the melting curve should not be great. The constants used are given in Tabie B-I and the results in Table B-II. The value of 1.5 for V_0/V corresponds to ~100 kbar in *Na*.

Table B-I

CONSTANTS USED IN EVALUATING EQUATIONS B-15 AND B-16 FOR SODIUM

QUANTITY	VALUE	REFERENCE
A	11.4 kbar	28[a]
a	3.56	28[a]
B	28 kbar	27[b]
b	3	27
T_{m0}	371°K	
$(\Delta V)_0$	12.2 cm^3/mole	26
$(\Delta G)_0$	7800 cal/mole	26
s	2.1	23

[a] These constants were derived by Gilvarry for <10 kb data, but reproduce fairly well the recent data of Newton *et al.* to 50 kbar.

[b] Chosen to give Amer. Inst. Phys. Hdbk. value for B_T (= bB).

Table B-II

CALCULATED RESULTS FOR SODIUM

V_0/V	$(\sigma_\infty/\sigma)\ \exp\ [(\Delta G)_0/kT_{m0}]$	
	Eq. B-15	Eq. B-16
1	1	1
1.1	17	1.4
1.2	160	2.9
1.5	30,000	46

The result is that the Keyes expression, Eq. B-9, with the experimentally determined exponent, indicates appreciably less variation of conductivity along the melting curve than does the arbitrary assumption of Eq. B-12.

The possibility was explored that a law of corresponding states might apply to ionic conduction. The difficulty here is that, although activation volumes have been determined for a number of solids, only in one or two cases has the pressure been raised high enough to measure any volume dependence of ΔV.[26,29] Available data do suggest the following:[23,24]

$$\frac{\Delta H}{T_m} = \text{constant for a given material} \quad . \tag{B-17}$$

Writing $\Delta G = \Delta H - T\Delta S$ in Eq. B-3a and with $T = T_m$:

$$\sigma = \sigma_\infty e^{+\Delta S/k}\ e^{-\Delta H/kT_m} \quad . \tag{B-18}$$

On the basis of Eq. B-17, all the volume dependence is in the entropy term, which is small[25] and expected to vary slowly.

A different approach is to look at the pressure dependence of diffusion or ionic conductivity in the molten state . Data have been found

for only two materials, Hg[30] and Ga.[31] In both cases, the activation volumes for diffusion are of the order of 5 percent of atomic volumes, much smaller than expected for solid material. That is, the pressure effect was found to be very small (as is also the case for the temperature effect) relative to that in solids. Now the conductivities of several molten salts have been measured at zero pressure by Yaffe and Van Artsdalen[20] and found to be of the order of $1(\Omega\text{-cm})^{-1}$. The temperature effect was very small—the activation energies (which varied somewhat with T) were in the range of 0.1 to 0.2 ev for NaCl, CsI, and KI, one order of magnitude lower than is observed in the solid state. Intuitively, we might then expect that for low enough pressures, the effect of pressure on the conductivity of molten salts would be small also. This is suggested by the observations on Hg and Ga and by Eq. B-8 if it is applicable to liquids. This latter question has been considered by Keyes[24] and, from an examination of viscosity data for isopropyl alcohol and a silicone trimer, he concludes that Eq. B-8 is satisfied only below 5 to 10 kbar. At higher pressure ΔV increased rather than decreased. This may merely indicate that activated-state theory is not applicable to viscosity in liquids.

In any event, we expect the resistivity of a molten salt to increase with increasing pressure, although the effect may be small. Hence, at high pressure in the vicinity of the melting curve, under equilibrium conditions, we would expect the alkali halides to have resistivities $> 1\Omega$-cm even if molten, and still greater if solid.

APPENDIX C

APPROXIMATE CORRECTION FOR NONUNIFORM SHOCK

APPENDIX C

APPROXIMATE CORRECTION FOR NONUNIFORM SHOCK

The explosive systems used in the present experiments, being finite in size, do not produce uniform shock waves; in other words, the pressure drops off behind the shock front rather than remaining constant. The rate of decay increases with increasing peak pressure.

It is only with the recent development in these laboratories of the Manganin-wire shock pressure gauge that a measurement of pressure profile has been possible. Peak pressures, as determined from free-surface velocity and/or impedance match measurements, were reported in Report I; in the present work, an attempt has been made to correct approximately for the pressure release behind the shock front. The procedure, chosen for simplicity consistent with the limited available data on pressure profiles and the uncertainty in calculating off-Hugoniot points, is described below.

For each explosive-driver plate assembly, a typical value of dP/dt (behind the front) was determined from gauge measurements made essentially at the surface of the driver (the gauge wire was actually displaced 1 mm from the surface). Using this slope and neglecting any attenuation of the peak pressure P_1, an average specimen pressure P' was deduced, corresponding to the time of measurement of resistance from the oscilloscope records. In order to estimate the volume and temperature corresponding to P', the isentrope along which the expansion occurs was approximated by the Hugoniot (see Figure C-1). The volume corresponding to P' is then V_2 and the corresponding temperature T_2^* is given by

$$T_2^* = T_1 e^{-a(V_2 - V_1)} \qquad \text{(C-1)}$$

where $a = \gamma/V$, γ being Grüneisen's ratio, and it is assumed that "a" is constant ($= \gamma_0/V_0$).†

† Equation C-1 expresses the variation of temperature with volume along any isentrope; in the present case the isentrope through P_1, V_1 has been approximated by the Hugoniot. The temperature T_2^*, corresponding to isentropic expansion from V_1 to V_2, will always exceed the temperature T_2 on the Hugoniot at volume V_2.

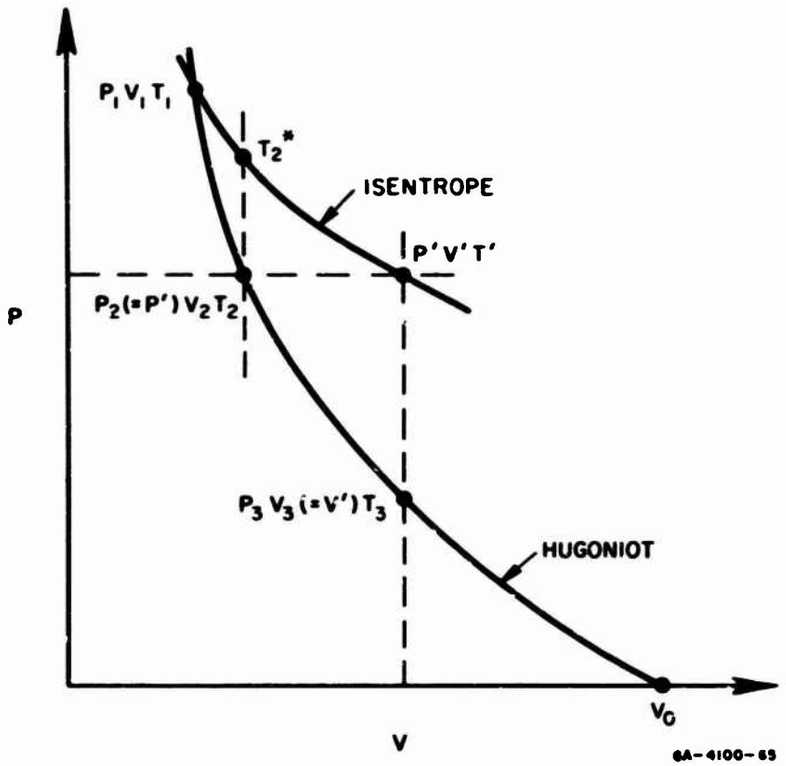

FIG. C-1 ESTIMATION OF POINT ON RELEASE ISENTROPE

Now, as indicated in Figure C-1, the "true" final state is P', V', T', and in the following discussion we estimate this state for comparison with $P_2 = P', V_2, T_2^*$. The worst case has been chosen—the highest pressure state which was produced by 9404 high explosive.

The problem is, given a Hugoniot curve along which P, V, and T are known, to determine V' and T' corresponding to a given P', the primed point lying on the isentrope through the point P_1, V_1, T_1 on the Hugoniot (see Figure C-1). Two equations in the unknowns V' and T' are

$$T' = T_1 e^{-a(V'-V_1)} \qquad \text{(C-2)}$$

$$P' - P_3(V') = (\partial P/\partial T)_V [T' - T_3(V')] \quad . \qquad \text{(C-3)}$$

We will assume

$$(\partial P/\partial T)_V = aC_V = \text{constant} \quad .$$

Eliminating T' from Eqs. C-2 and C-3 yields

$$P' - Be^{-aV'} = P_3(V') - AT_3(V') \qquad \text{(C-4)}$$

where

$$A \equiv aC_v \quad \text{and} \quad B \equiv AT_1 e^{aV_1} \quad .$$

Equation C-4 was solved for V' by plotting the left and right sides of the equation against V' as a variable and finding the intersection of the resulting curves. T' was then determined from Eq. C-2. A comparison of values for the worst case (*i.e.*, where the corrections are largest) is as follows:

Peak values:	P_1 = 340 kbar ,	V_1 = 0.1290 cm^3/g ,	T_1 = 5780°K
"Corrected" values:	P' = 298 kbar ,	V_2 = 0.1325 cm^3/g ,	T_2^* = 5600°K
			(T_2 = 4630°K)
"True" values:	P' = 298 kbar ,	V' = 0.1346 cm^3/g ,	T' = 5500°K

Thus the volume correction is about 38 percent too small and the temperature correction about 36 percent too small. That is, the corrected values of volume and temperature are ~1.6 percent too low and 1.1 percent too high, respectively. The latter discrepancy is insignificant with respect to the absolute uncertainty in calculated temperatures.

APPENDIX D

DERIVATION OF EQUATION (9) FOR RESISTIVITY OF A POLAR SEMICONDUCTOR

APPENDIX D

DERIVATION OF EQUATION (9) FOR RESISTIVITY OF A POLAR SEMICONDUCTOR

For an intrinsic semiconductor with equal concentrations n and equal mobilities μ of electrons and holes, the conductivity σ is given by

$$\sigma = 2ne\mu \qquad \text{(D-1)}$$

where e is the electronic charge and μ the mobility. Writing explicitly the expression for n in Eq. (D-1) yields

$$\sigma = 4e(2\pi mkT/h^2)^{3/2}e^{-Eg/2kT}\mu \quad . \qquad \text{(D-2)}$$

For polar semiconductors[32] it is found that the mobility depends on temperature as

$$\mu = \mu_0 T^{-n} \qquad \text{(D-3)}$$

where n usually lies between 2 and 3; let $n = 2.5$. We will evaluate μ_0 by fitting Eq. (D-3) to a typical value of mobility, *viz.*, 100 cm^2/v-sec at $T = 500°K$.[32] Hence $\mu_0 = 5.6 \times 10^8$ $cm^2 deg^{2.5}$/v-sec. Then

$$\sigma = (B/T)e^{-Eg/2kT} \qquad \text{(D-4)}$$

where

$$B \equiv 4e\mu_0(2\pi mk/h^2)^{3/2} = 0.85 \times 10^6 \ °K/\Omega\text{-cm} \quad .$$

Or, since

$$\rho = 1/\sigma \ , \quad \rho = (1.2 \times 10^{-6})Te^{Eg/2kT} \quad . \qquad \text{(D-5)}$$

APPENDIX E

DISCUSSION OF PHASE CHANGES IN SODIUM CHLORIDE

APPENDIX E

DISCUSSION OF PHASE CHANGES IN SODIUM CHLORIDE

Evdokimova and Vereshchagin[32] have recently reported a crystal structure change in NaCl at 17 kbars using high-pressure X-ray methods. They report the high pressure phase has a CsCl structure with a volume change of 14.9 percent and that no more than 5 percent of the substance transforms during 10 to 20 hours at ~19 kbar. They also state that the high-pressure phase is usually preserved after the release of pressure. These facts indicate an extremely sluggish transition.

Pistorius[34] states that Piermarini and Weir were unsuccessful in corroborating the transition, possibly due to its sluggishness. Bassett and Takahashi[35] also failed to corroborate the transition. However, Pistorius[34] has succeeded in verifying this transition and in addition has measured its temperature dependence to 220°C.[34] He indicates that the transition is sharper at the higher temperatures.

Recently Larson at the Lawrence Radiation Laboratory at Livermore[36] has observed what he believes to be a multiwave shock front in single crystal NaCl using a quartz transducer. He is tentatively suggesting that this multiwave structure is due to the transition observed by Pistorius. His preliminary data place the transition at 29 kbars.

Alder[13] has published data indicating a break in the Hugoniot which he suggested was a transformation from the NaCl to the CsCl type structure. The pressure of the transition was originally given as approximately 300 kbar. However, a recent revision of the data[36] has placed this transition at about 220 kbar. The exact pressure seems to differ by 10 or 20 kbar depending on the crystal orientation.[36]

This transition has been confirmed qualitatively for the [100] direction by Hauver and Melani[37] who are presently studying it as a function of crystal orientation.

If the preliminary observation by Larson is substantiated, then two transitions occur in NaCl under shock. Larson suggests that the transition at about 240 kbar may be melting.[36]

This melting hypothesis is not consistent with extrapolation of the melting curve shown in Figure 21, which indicates a melting temperature at 250 kbar of about 3000°K; the calculated shock temperature at 250 kbar is only about 1200°K. However, the validity of such a long extrapolation of the static melting data is highly questionable; indeed, if the low-pressure transition is occurring, the extrapolation is for the wrong phase.

ACKNOWLEDGMENTS

The assistance of Paul S. DeCarli and Arlon Hunt with the heated crystal shots is gratefully acknowledged.

REFERENCES

1. Alder, B. J. and R. H. Christian, "Metallic Transition in Ionic and Molecular Crystals," *Phys. Rev. 104*, 550-551 (1956). "Pressure Induced Metallic Transitions in Insulators," *Discussions Faraday Soc.*, **22**, 44 (1956).

2. Doran, D. G. and T. J. Ahrens, "Electrical Effects of Shock Waves: Conductivity in CsI and KI. Thermoelectric Measurements in Metals," Stanford Research Institute, Project 4100, Final Report, 1963.

3. Griggs, D. T., W. G. McMillan, E. D. Michael, and C. P. Nash, "Lack of Metallic Transitions in LiH and $LiAlH_4$ under Static Pressure," *Phys. Rev. 109*, 1858 (1958).

4. Drickamer, H. G., private communication.

5. Flower, M. and N. H. March, "Transitions to Metallic States in Ionic Crystals, with Particular Reference to Cesium Iodide," *Phys. Rev. 125*, 1144-1146 (1962).

6. Bernstein, D. and D. C. Keough, "Piezoresistivity of Manganin," *J. Appl. Phys. 35*, 1471-1474 (1964).

7. Eichelberger, R. J. and G. E. Hauver, "Solid State Transducers for Recording of Intense Pressure Pulses," *Les Ondes de Detonations*, Editions de Centre Nationale de la Recherche Scientifique, 15 Quai Avatole-France, Paris (VII^e), 3o3-381 (1962).

8. Christian, R. H., "The Equation of State of the Alkali Halides at High Pressure," doctoral thesis, University of California Report No. UCRL-4900, 1957.

9. Walsh, J. M., M. H. Rice, R. G. McQueen, and F. L. Yarger, "Shock-Wave Compression of Twenty-Seven Metals, Equations of State of Metals," *Phys. Rev. 108*, 196-216 (1957).

10. Al'tshuler, L. V., L. V. Kuleshova, and M. N. Pavlovskii, "The Dynamic Compressibility, Equation of State, and Electrical Conductivity of Sodium Chloride at High Pressures," *Soviet Physics-JETP 12*, 10-15 (1961).

11. Walsh, J. M and R. H. Christian,"Equation of State of Metals from Shock Wave Measurements," *Phys. Rev. 97*, 1544 (1955).

12. Al'tshuler, L. V., M. N. Pavlovskii, L. V. Kuleshova, and G. V. Simakov, "Investigation of Alkali-Metal Halides at High Pressures and Temperatures Produced by Shock Compression," *Soviet Physics-Solid State 5*, 203-211 (1963).

13. Alder, B. J., "Physics Experiments with Strong Pressure Pulses," *Solids under Pressure*, W. Paul and D. M. Warschauer, eds., McGraw-Hill, N. Y., 1963, pp. 385-420.

14. Etzel, H. W. and R. J. Maurer, "The Concentration and Mobility of Vacancies in Sodium Chloride," *J. Chem. Phys. 18*, 1003-1007 (1950).

15. Lynch, David W., "Diffusion and Ionic Conductivity in Cesium Bromide and Cesium Iodide," *Phys. Rev. 118*, 468 (1960).

16. Pierce, C. B., "Effect of Pressure on the Ionic Conductivity in Doped Single Crystals of NaCl, KCl, and RbCl, "Phys. Rev. 123, *744 (1961)*.

17. Lidiard, A. B., "Ionic Conductivity," *Encyclopedia of Physics*, S. Flugge, ed., Springer-Verlag, Berlin, 1957, Vol. 20, pp. 246-349.

18. Clark, S. B., Jr., "Effect of Pressure on the Melting Points of Eight Alkali Halides," *J. Chem. Phys. 31*, 1526-1531 (1959).

19. Bundy, F. P. and H. M. Strong, "Behavior of Metals at High Temperatures and Pressure," *Solid State Physics*, F. Seitz and D. Turnbull, eds., Academic Press, N. Y., 1962, Vol. 13, p. 140.

20. Yaffe, I. S. and E. R. Van Artsdalen, "Electrical Conductance and Density of Pure Molten Alkali Halides," *J. Phys. Chem. 60*, 1125 (1956).

21. Grantham, L. F., "Negative-Temperature Coefficients of Electrical Conductivity in Fused Salts," *Bull. Amer. Phys. Soc. II 9*, 534 (1964).

22. Lazarus, David, "Effect of High Pressure on Diffusion," *Solids under Pressure*, W. Paul and D. M. Warschauer, eds., McGraw-Hill, New York, 1963, pp. 43-69.

23. Keyes, Robert W., "Volumes of Activation, II. Pressure Dependence of Activation Parameters," *J. Chem. Phys. 32*, 1066-7 (1960).

24. Keyes, Robert W., "Continuum Models of the Effect of Pressure on Activated Processes," *Solids under Pressure*, W. Paul and D. M. Warschauer, eds., McGraw-Hill, New York, 1963, pp. 71-99.

25. Murnaghan, F. D., *Finite Deformation of an Elastic Solid*, Wiley, New York, 1951.

26. Nachtrieb, N. H., J. A. Weil, E. Catalano, and L. W. Lawson, "Self-Diffusion in Solid Sodium, II. The Effect of Pressure," *J. Chem. Phys. 20*, 1189-94 (1952).

27. Bridgman, P. W., "The Compression of 39 Substances to 100,000 Kg/cm^2," *Proc. Am. Acad. Arts Sci. 76*, 55-87 (1948).

28. Constants are those fit to < 10 kbar data by Gilvarry, quoted in Ref. 19, pp. 134. For the present purpose they give adequate fit to the more recent data of R. C. Newton, A. Jayaraman and G. C. Kennedy, "The Fusion Curves of the Alkali Metals to 50 kbar." *J. Geophys. Res. 67*, 2559 (1962).

29. Nachtrieb, N. and A. W. Lawson, "Effect of Pressure on Self-Diffusion in White Phosphorus," *J. Chem. Phys. 23*, 1193-95 (1955).

30. Nachtrieb, N. H. and Jean Petit, "Self-Diffusion in Liquid Mercury," *J. Chem. Phys. 24*, 746-50 (1956).

31. Petit, Jean and N. H. Nachtrieb, "Self-Diffusion in Liquid Gallium," *J. Chem. Phys. 24*, 1027-8 (1956).

32. Scanlon, W. W., "Polar Semiconductors," *Solid State Physics*, F. Seitz and D. Turnbull, eds., Academic Press, N. Y., 1959, Vol 13, p. 83.

33. Evdokimova, V. V. and Vereshchagin, "Polymorphic Transition in Sodium Chloride under Pressure," *Soviet Physics—Solid State 4*, 1438 (1963).

34. Pistorius, Carl W. F. T., "Polymorphic Transitions of the Alkali Chlorides at High Pressures to 200°C," *J. Phys. Chem. Solids 25*, 1477 (1964).

35. Bassett, W. A. and T. Takahashi, "Specific Volume Measurements of Crystalline Solids at Pressures up to 200 Kilobars by X-Ray Diffraction," ASME Paper 64-WA/PT-24, presented at Winter Annual Meeting, Dec., 1964.

36. Larson, Donald B., Lawrence Radiation Laboratory, Livermore, California, private communication.

37. Hauver, G. E. and A. Melani, Ballistics Research Laboratory, Aberdeen, Maryland, private communication.